

Convergence analysis of three semi-discrete numerical schemes for nonlocal geometric flows including perimeter terms

Wei, Jiang*

Chunmei, Su[†]Ganghui, Zhang[‡]

May 14, 2024

Abstract

We present and analyze three distinct semi-discrete schemes for solving nonlocal geometric flows incorporating perimeter terms. These schemes are based on the finite difference method, the finite element method, and the finite element method with a specific tangential motion. We offer rigorous proofs of quadratic convergence under H^1 -norm for the first scheme and linear convergence under H^1 -norm for the latter two schemes. All error estimates rely on the observation that the error of the nonlocal term can be controlled by the error of the local term. Furthermore, we explore the relationship between the convergence under L^∞ -norm and manifold distance. Extensive numerical experiments are conducted to verify the convergence analysis, and demonstrate the accuracy of our schemes under various norms for different types of nonlocal flows.

MSCcodes: 65M60, 65M12, 35K55

Keywords: Nonlocal geometric flows; Finite difference method; Finite element method; Tangential motion; Error analysis; Manifold distance

1 Introduction

In this paper, we analyze and establish the convergence result of three distinct numerical methods for evolving a closed plane curve $\Gamma(t)$ under a nonlocal flow that involves perimeter. The normal velocity of $\Gamma(t)$ is determined by the formula

$$\mathcal{V} = (\kappa - f(L))\mathcal{N}, \quad (1.1)$$

where κ represents the curvature of the curve, f is a Lipschitz function, L is the perimeter, and \mathcal{N} is the unit inner normal vector. Equation (1.1) encompasses a wide range of geometric

*School of Mathematics and Statistics, Wuhan University, Wuhan, 430072, China (jiangwei1007@whu.edu.cn).

[†]Yau Mathematical Sciences Center, Tsinghua University, Beijing, 100084, China(sucm@tsinghua.edu.cn).

[‡]Yau Mathematical Sciences Center, Tsinghua University, Beijing, 100084, China(gh-zhang19@mails.tsinghua.edu.cn).

flows, including:

$$f(L) = \begin{cases} \frac{2\pi}{L}, & \text{for area-preserving curve shortening flow of simple curves [23] ,} \\ \frac{2\pi \operatorname{ind}(\Gamma)}{L}, & \text{for area-preserving curve shortening flow of nonsimple curves [41],} \\ \frac{2\pi-\beta}{L}, & \text{for curve flows with a prescribed rate of change of area [11, 39],} \end{cases}$$

where $\beta \in (-\infty, \infty)$, $\operatorname{ind}(\Gamma) \in \mathbb{Z}$ denotes the rational index [19] of a nonsimple curve Γ . The inclusion of an additional nonlocal force, $f(L)$, enables us to control the area change of an evolving curve. Indeed, by the theorem of turning tangents [19], the rate of area change can be determined by [13]

$$\frac{dA}{dt} = \int_{\Gamma} \mathcal{V} \cdot \mathcal{N} ds = \begin{cases} 0, & \text{for } f(L) = \frac{2\pi}{L} \text{ and simple curves,} \\ 0, & \text{for } f(L) = \frac{2\pi \operatorname{ind}(\Gamma)}{L} \text{ and nonsimple curves,} \\ -\beta, & \text{for } f(L) = \frac{2\pi-\beta}{L} \text{ and simple curves.} \end{cases}$$

In this paper, we focus on the study of curve evolutions that maintain their topological characteristics.

In recent years, there has been significant emphasis on the development of theoretical and modeling frameworks for nonlocal geometric flows. One prominent instance of such work is the area-preserving curve shortening flow (AP-CSF), which has become vital in the field of image processing [24, 36, 35] and can be interpreted as a limit of the nonlocal model of the Ginzburg-Laudau equation [7]. The existence and convergence results of AP-CSF for both simple and nonsimple closed curve cases have been extensively explored [23, 41]. Moreover, the study of curve flows with a prescribed rate of change in the enclosed area has arisen in connection with the investigation of contracting bubbles in fluid mechanics [9, 10, 11], and the long-time behavior of such flows has been addressed in [39]. For more comprehensive theoretical studies related with nonlocal geometric flows, we refer to [8, 25, 38].

Extensive numerical methods have been employed to simulate the AP-CSF and curve flows with a prescribed rate of change in the enclosed area. Examples of such methods for the AP-CSF include the finite difference method [29], the MBO method [34], the crystalline algorithm [40], as well as PFEMs [32, 6]. Additionally, a rescaled spectral collocation scheme was proposed in [11] for closed embedded plane curves with a prescribed rate of change in the enclosed area. However, there has been relatively little research on the numerical analysis of these methods. Recently, in [26], the authors proposed a semi-discrete finite element method for the AP-CSF of simple curves and established its convergence in H^1 -norm. The nonlocal nature of the geometric equations presents a major challenge for the error analysis.

In this paper, we propose three numerical schemes for nonlocal geometric flows involving perimeter (1.1) and give their error estimates. Our main observation is that the difference between the nonlocal term and its discrete version can be managed through the disparity of the local term. Specifically, we introduce the following three different types of semi-discrete schemes:

- Firstly, we employ a finite difference method to discretize the parametrization equation

of (1.1)

$$\partial_t X = \frac{1}{|\partial_\xi X|} \partial_\xi \left(\frac{\partial_\xi X}{|\partial_\xi X|} \right) - f(L) \left(\frac{\partial_\xi X}{|\partial_\xi X|} \right)^\perp, \quad \xi \in \mathbb{S}^1, \quad (1.2)$$

where $\mathbb{S}^1 = [0, 2\pi]$, $(a, b)^\perp := (-b, a)$ denotes a clockwise rotation by $\pi/2$ and the periodic function $X(\xi, t) : \mathbb{S}^1 \times [0, T] \rightarrow \mathbb{R}^2$ is a parameterization of the closed curve $\Gamma \subset \mathbb{R}^2$. Under certain appropriate assumptions, we demonstrate that the resulting semi-discrete scheme converges quadratically in the discrete H^1 -norm as defined in [15]. The proof is based on a careful Taylor expansion result and an averaged approximation of the normal vector.

- Secondly, we utilize a finite element method for a natural weak formulation of (1.2). The derived semi-discrete scheme is based on our previous work on AP-CSF of simple curves [26]. An H^1 -optimal error estimate follows from our key observation mentioned above.
- Thirdly, we introduce an artificial tangential motion and apply a finite element method for an alternative parametrization of the geometric equation

$$\partial_t X = \frac{\partial_{\xi\xi} X}{|\partial_\xi X|^2} - f(L)\mathcal{N}. \quad (1.3)$$

This form of reparametrization was initially proposed by Deckelnick and Dziuk for the curve shortening flow [12] to improve the mesh quality during evolution. It was later interpreted as a DeTurck trick by Elliot and Fritz in [22]. Recently, the DeTurck trick has been further applied to various geometric flows such as elastic flow [33], anisotropic curve shortening flow [17, 16, 14] and fourth-order flows [18]. We emphasize that we have successfully extended the DeTurck trick to the general nonlocal flow case. The resulting semi-discrete scheme yields an asymptotic equidistribution property, as well as an H^1 -optimal error estimate.

As a byproduct, we further explore the convergence of the schemes under manifold distance, a topic extensively discussed in the numerical computation community [4, 5, 42, 27, 28]. We prove that, for simple curves, convergence in the function L^∞ -norm implies convergence under the manifold distance. Moreover, we prove an optimal convergence of the finite difference scheme under the manifold distance.

The rest of this paper is organized as follows. In Section 2, we briefly introduce the mathematical notations. In Section 3, we propose the semi-discrete schemes and provide the error estimates for the finite difference method. In Section 4, we consider the finite element method, and the finite element method with a tangential motion. Section 5 aims to establishing a connection between the convergence of the manifold distance and L^∞ -norm. Section 6 presents extensive numerical experiments for the three different numerical schemes and various types of nonlocal flows. The numerical results demonstrate our convergence analysis results in both the H^1 -norm and the manifold distance. Moreover, a better mesh quality is achieved for the finite element method with the aid of tangential motions. Finally, we draw some conclusions in Section 7.

2 Notations

Throughout the paper, we denote the quantities related to the real solution and discrete solution by capital and lower-case letters, respectively. Specifically, for the solution of (1.2), we denote $\mathcal{T} = \frac{\partial_\xi X}{|\partial_\xi X|}$ and $\mathcal{N} = \mathcal{T}^\perp$ by the tangent and inner normal of the curve, respectively. Thus (1.2) can be simply written as

$$\partial_t X = \frac{1}{|\partial_\xi X|} \partial_\xi \mathcal{T} - f(L) \mathcal{N}, \quad \xi \in \mathbb{S}^1; \quad X(\xi, 0) = X^0(\xi). \quad (2.1)$$

Direct computation gives

$$\partial_t |\partial_\xi X| = \partial_t \partial_\xi X \cdot \mathcal{T} = \partial_\xi (\partial_t X \cdot \mathcal{T}) - \partial_t X \cdot \partial_\xi \mathcal{T} = -|\partial_\xi X| |\partial_t X|^2 - f(L) |\partial_\xi X| \partial_t X \cdot \mathcal{N}. \quad (2.2)$$

For spatial discretization, we utilize a uniform mesh, where the equidistributed grid points $\mathcal{G}_h := \{\xi_1, \dots, \xi_N\} \subset \mathbb{S}^1$ are given by $\xi_j = jh, j = 0, \dots, N$ for $h = 2\pi/N$ with $N \geq 2$. We use a periodic index, i.e., $a_j = a_{j \pm N}$ when involved. Denote $X_j = X(\xi_j)$, $\dot{X}_j = \partial_t X(\xi_j)$, and set

$$Q_j = |X_j - X_{j-1}|, \quad \mathcal{T}_j = \frac{X_j - X_{j-1}}{Q_j}, \quad j = 1, \dots, N.$$

Let $x_h : \mathcal{G}_h \rightarrow \mathbb{R}^2$ be a grid function. We define the discrete length element q_j , the discrete tangent τ_j and normal n_j as

$$q_j = |x_j - x_{j-1}|, \quad \tau_j = \frac{x_j - x_{j-1}}{q_j}, \quad n_j = \tau_j^\perp, \quad (2.3)$$

where $x_j = x_h(\xi_j)$ denotes the vertex of the polygon that approximates the curve. Denote $l_h = \sum_{j=1}^N q_j$ by the perimeter of the polygon. Throughout the article, we denote C by a general constant which is independent of the mesh size h and might vary from line to line.

(Assumption 2.1) Suppose that the solution of (1.2) satisfies $X \in C^1([0, T], C^4(\mathbb{S}^1))$, i.e.,

$$K_1(X) := \|X\|_{C^1([0, T], C^4(\mathbb{S}^1))} < \infty,$$

and there exist constants $0 < C_1 < C_2$ such that

$$C_1 \leq |\partial_\xi X(\xi, t)| \leq C_2, \quad \forall (\xi, t) \in \mathbb{S}^1 \times [0, T]. \quad (2.4)$$

Under this assumption, we have the following results, which have been established in [15].

Lemma 2.1 [15, Lemmas 3.1, 3.3] *Under Assumption 2.1, there exists $h_0 > 0$ such that for $0 < h \leq h_0$, we have*

$$C_1 \leq Q_j/h \leq C_2, \quad \frac{Q_j + Q_{j+1}}{2h} = |\partial_\xi X(\xi_j)| + O(h^2), \quad (2.5a)$$

$$\mathcal{T}_j + \mathcal{T}_{j+1} = 2\mathcal{T}(\xi_j) + O(h^2), \quad \mathcal{T}_j = \frac{1}{2}(\mathcal{T}(\xi_j) + \mathcal{T}(\xi_{j-1})) + O(h^2), \quad (2.5b)$$

$$\frac{\mathcal{T}_{j+1} - \mathcal{T}_j}{h} = \partial_\xi \mathcal{T}(\xi_j) + O(h^2), \quad \frac{\dot{X}_{j+1} - \dot{X}_j}{h} = \frac{1}{2} (\partial_t \partial_\xi X(\xi_j) + \partial_t \partial_\xi X(\xi_{j+1})) + O(h^2), \quad (2.5c)$$

$$\left| \tau_{j+1/2}^\perp - \mathcal{N}(\xi_j) \right| \leq \frac{2}{|\mathcal{T}_j + \mathcal{T}_{j+1}|} (|\mathcal{T}_j - \tau_j| + |\mathcal{T}_{j+1} - \tau_{j+1}|) + Ch^2, \quad (2.5d)$$

where $\tau_{j+1/2} := \frac{\tau_j + \tau_{j+1}}{|\tau_j + \tau_{j+1}|}$ represents the averaged vertex tangent.

For a grid function $u : \mathcal{G}_h \rightarrow \mathbb{R}^2$, we define the backward difference quotient as

$$\delta u_j := \frac{u_j - u_{j-1}}{h}, \quad j = 1, \dots, N.$$

Moreover, to measure the error, we introduce the following discrete norms:

$$\|u\|_{L_G^2} := \left(h \sum_{j=1}^N |u_j|^2 \right)^{\frac{1}{2}}, \quad \|u\|_{H_G^1} := \left(h \sum_{j=1}^N (|u_j|^2 + |\delta u_j|^2) \right)^{\frac{1}{2}}. \quad (2.6)$$

3 Finite difference method

In this section, we utilize a finite difference method to solve the equation (1.2).

Definition 3.1 A semi-discrete finite difference approximation of (1.2) is to find a grid function $x_h : \mathcal{G}_h \times [0, T] \rightarrow \mathbb{R}^2$ such that

$$\dot{x}_j = \frac{2}{q_j + q_{j+1}} (\tau_{j+1} - \tau_j) - f(l_h) \tau_{j+1/2}^\perp \quad \text{in} \quad (0, T]; \quad x_j(0) = X^0(\xi_j). \quad (3.1)$$

Theorem 3.2 Let $X(\xi, t)$ be a solution of (1.2) satisfying Assumption 2.1. Then there exists $h_0 > 0$ such that for all $0 < h \leq h_0$, there exists a unique finite difference semi-discrete solution $x_h(t)$ in the sense of (3.1). Furthermore, we have the following error estimate

$$\sup_{t \in [0, T]} \|X(t) - x_h(t)\|_{H_G^1} \leq Ch^2, \quad (3.2)$$

where the constants h_0, C depend on $C_1, C_2, K_1(X), T$ and f .

First, we compute the evolution equation for the discrete length q_j .

Lemma 3.3 Suppose x_h is the finite difference semi-discrete solution in the sense of (3.1), then we have

$$\dot{q}_j + \frac{q_{j-1} + q_j}{4} |\dot{x}_{j-1}|^2 + \frac{q_j + q_{j+1}}{4} |\dot{x}_j|^2 + \frac{q_{j-1} + q_j}{4} f(l_h) \dot{x}_{j-1} \cdot \tau_{j-1/2}^\perp + \frac{q_{j+1} + q_j}{4} f(l_h) \dot{x}_j \cdot \tau_{j+1/2}^\perp = 0. \quad (3.3)$$

Proof We begin by computing \dot{q}_j as

$$\begin{aligned} \dot{q}_j &= (\dot{x}_j - \dot{x}_{j-1}) \cdot \tau_j \\ &= \tau_j \cdot \left(\frac{2}{q_j + q_{j+1}} (\tau_{j+1} - \tau_j) - f(l_h) \tau_{j+1/2}^\perp - \frac{2}{q_j + q_{j-1}} (\tau_j - \tau_{j-1}) + f(l_h) \tau_{j-1/2}^\perp \right) \\ &= \frac{2}{q_j + q_{j+1}} (\tau_j \cdot \tau_{j+1} - 1) - f(l_h) \tau_{j+1/2}^\perp \cdot \tau_j - \frac{2}{q_j + q_{j-1}} (1 - \tau_j \cdot \tau_{j-1}) + f(l_h) \tau_{j-1/2}^\perp \cdot \tau_j \\ &= \frac{2}{q_j + q_{j+1}} (\tau_j \cdot \tau_{j+1} - 1) - f(l_h) \tau_{j+1/2}^\perp \cdot \tau_j + \frac{2}{q_j + q_{j-1}} (\tau_j \cdot \tau_{j-1} - 1) - f(l_h) \tau_{j-1/2}^\perp \cdot \tau_{j-1} \\ &=: J_j + J_{j-1}, \end{aligned} \quad (3.4)$$

where for the last second equality, we have employed the property

$$\tau_{j-1/2}^\perp \cdot \tau_j = \tau_{j-1}^\perp / |\tau_j + \tau_{j-1}| \cdot \tau_j = -\tau_{j-1} \cdot \tau_j^\perp / |\tau_j + \tau_{j-1}| = -\tau_{j-1} \cdot \tau_{j-1/2}^\perp. \quad (3.5)$$

Multiplying (3.1) by $\frac{q_j + q_{j+1}}{4} f(l_h) \tau_{j+1/2}^\perp$, we obtain

$$\frac{q_j + q_{j+1}}{4} f(l_h) \tau_{j+1/2}^\perp \cdot \dot{x}_j + \frac{q_j + q_{j+1}}{4} f(l_h)^2 - f(l_h) \tau_{j+1/2}^\perp \cdot \frac{\tau_{j+1} - \tau_j}{2} = 0,$$

which can be simplified as

$$\frac{q_j + q_{j+1}}{4} f(l_h) \tau_{j+1/2}^\perp \cdot \dot{x}_j + \frac{q_j + q_{j+1}}{4} f(l_h)^2 + f(l_h) \tau_{j+1/2}^\perp \cdot \tau_j = 0, \quad (3.6)$$

by using (3.5). Combining (3.1) and (3.6), we get

$$\begin{aligned} J_j &= \frac{2}{q_j + q_{j+1}} \left(-\frac{1}{2} |\tau_j - \tau_{j+1}|^2 \right) - f(l_h) \tau_{j+1/2}^\perp \cdot \tau_j \\ &= -\frac{1}{q_j + q_{j+1}} \left| \dot{x}_j + f(l_h) \tau_{j+1/2}^\perp \right|^2 \left(\frac{q_j + q_{j+1}}{2} \right)^2 - f(l_h) \tau_{j+1/2}^\perp \cdot \tau_j \\ &= -\frac{q_j + q_{j+1}}{4} \left(|\dot{x}_j|^2 + 2f(l_h) \tau_{j+1/2}^\perp \cdot \dot{x}_j + f(l_h)^2 \right) - f(l_h) \tau_{j+1/2}^\perp \cdot \tau_j \\ &= -\frac{q_j + q_{j+1}}{4} |\dot{x}_j|^2 - \frac{q_j + q_{j+1}}{2} f(l_h) \tau_{j+1/2}^\perp \cdot \dot{x}_j - \frac{q_j + q_{j+1}}{4} f(l_h)^2 - f(l_h) \tau_{j+1/2}^\perp \cdot \tau_j \\ &= -\frac{q_j + q_{j+1}}{4} |\dot{x}_j|^2 - \frac{q_j + q_{j+1}}{4} f(l_h) \tau_{j+1/2}^\perp \cdot \dot{x}_j. \end{aligned}$$

Plugging this into (3.4) yields (3.3), and the proof is completed. \square

Proof [Proof of Theorem 3.2] We define

$$T^* = \sup \left\{ t \in [0, T] : x_h \text{ solves (3.1) with } \frac{C_1}{2} \leq \frac{q_j(t)}{h} \leq 2C_2, \max_{j=1, \dots, N} |\mathcal{T}_j(t) - \tau_j(t)| \leq h^{\frac{5}{4}} \right\}. \quad (3.7)$$

Clearly $T^* > 0$. Noticing the nonlinear terms in (3.1) are locally Lipschitz with respect to x_j , we get local existence and uniqueness using standard ODE theory. Furthermore, since $q_j(0) = Q_j(0)$ and $\tau_j(0) = \mathcal{T}_j(0)$, the desired estimate also holds by continuity. By (3.7) and the Lipschitz continuity of f , we have $\forall t \in [0, T^*]$,

$$2\pi C_1 \leq L \leq 2\pi C_2, \quad \pi C_1 \leq l_h \leq 4\pi C_2, \quad |f(L)| \leq C, \quad (3.8)$$

where C is a constant depending on C_1, C_2 and f . We claim that there exists a constant $h_1 > 0$ such that for $0 < h \leq h_1$, it holds

$$\max_{j=1, \dots, N} |\dot{x}_j(t)| \leq C, \quad \forall t \in [0, T^*], \quad (3.9)$$

where C depends on C_1, C_2 and f . Indeed, by (3.1), (2.5c), (3.7) and (3.8), we obtain

$$\begin{aligned} |\dot{x}_j|^2 &\leq 2 \left| \frac{2}{q_j + q_{j+1}} (\tau_{j+1} - \tau_j) \right|^2 + 2 \left| f(l_h) \tau_{j+1/2}^\perp \right|^2 \leq C \left| \frac{\tau_{j+1} - \tau_j}{h} \right|^2 + C \\ &\leq C \left(\left| \frac{\mathcal{T}_{j+1} - \mathcal{T}_j}{h} \right| + \frac{2}{h} \max_{k=1, \dots, N} |\mathcal{T}_k - \tau_k| \right)^2 + C \leq C. \end{aligned}$$

Moreover, based on (2.5b), we have

$$\min_{j=1,\dots,N} |\mathcal{T}_j + \mathcal{T}_{j+1}| \geq 1, \quad (3.10)$$

when h is sufficiently small. Define the truncation error as

$$\mathcal{R}_j := \dot{X}_j - \frac{2}{Q_j + Q_{j+1}} (\mathcal{T}_{j+1} - \mathcal{T}_j) + f(L)\mathcal{N}(\xi_j), \quad (3.11)$$

$$\begin{aligned} \tilde{\mathcal{R}}_j &:= \dot{Q}_j + \frac{Q_{j-1} + Q_j}{4} |\dot{X}_{j-1}|^2 + \frac{Q_j + Q_{j+1}}{4} |\dot{X}_j|^2 \\ &\quad + \frac{Q_{j-1} + Q_j}{4} f(L) \dot{X}_{j-1} \cdot \mathcal{N}(\xi_{j-1}) + \frac{Q_{j+1} + Q_j}{4} f(L) \dot{X}_j \cdot \mathcal{N}(\xi_j). \end{aligned} \quad (3.12)$$

(1). *Estimates of the truncation error $\mathcal{R}_j, \tilde{\mathcal{R}}_j$.* Employing (1.2), (2.5a) and (2.5c), one gets

$$\begin{aligned} \mathcal{R}_j &= \dot{X}_j - \frac{2}{Q_j + Q_{j+1}} (\mathcal{T}_{j+1} - \mathcal{T}_j) + f(L)\mathcal{N}(\xi_j) \\ &= \dot{X}_j - \frac{1}{|\partial_\xi X(\xi_j)| + O(h^2)} (\partial_\xi \mathcal{T}(\xi_j) + O(h^2)) + f(L)\mathcal{N}(\xi_j) \\ &= \dot{X}_j - \frac{1}{|\partial_\xi X(\xi_j)|} (1 + O(h^2)) \cdot (\partial_\xi \mathcal{T}(\xi_j) + O(h^2)) + f(L)\mathcal{N}(\xi_j) \\ &= \dot{X}_j - \frac{1}{|\partial_\xi X(\xi_j)|} \partial_\xi \mathcal{T}(\xi_j) + f(L)\mathcal{N}(\xi_j) + O(h^2) \\ &= O(h^2). \end{aligned} \quad (3.13)$$

Similarly, applying (2.2), (2.5b) and (2.5c), we derive

$$\begin{aligned} \dot{Q}_j &= (\dot{X}_j - \dot{X}_{j-1}) \cdot \mathcal{T}_j \\ &= \frac{h}{4} (\partial_t \partial_\xi X(\xi_{j-1}) + \partial_t \partial_\xi X(\xi_j)) \cdot (\mathcal{T}(\xi_j) + \mathcal{T}(\xi_{j-1})) + O(h^3) \\ &= \frac{h}{2} \partial_t \partial_\xi X(\xi_{j-1}) \cdot \mathcal{T}(\xi_{j-1}) + \frac{h}{2} \partial_t \partial_\xi X(\xi_j) \cdot \mathcal{T}(\xi_j) + O(h^3) \\ &= \frac{h}{2} (-|\partial_\xi X| |\partial_t X|^2(\xi_{j-1}) - f(L) |\partial_\xi X|(\xi_{j-1}) \partial_t X(\xi_{j-1}) \cdot \mathcal{N}(\xi_{j-1})) \\ &\quad + \frac{h}{2} (-|\partial_\xi X| |\partial_t X|^2(\xi_j) - f(L) |\partial_\xi X|(\xi_j) \partial_t X(\xi_j) \cdot \mathcal{N}(\xi_j)) + O(h^3), \end{aligned}$$

which together with (2.5a) implies

$$\begin{aligned} \tilde{\mathcal{R}}_j &= \dot{Q}_j + \frac{Q_{j-1} + Q_j}{4} |\dot{X}_{j-1}|^2 + \frac{Q_j + Q_{j+1}}{4} |\dot{X}_j|^2 \\ &\quad + \frac{Q_{j-1} + Q_j}{4} f(L) \dot{X}_{j-1} \cdot \mathcal{N}(\xi_{j-1}) + \frac{Q_{j+1} + Q_j}{4} f(L) \dot{X}_j \cdot \mathcal{N}(\xi_j) = O(h^3). \end{aligned} \quad (3.14)$$

(2). *Stability.* Denote $e_j(t) = X_j(t) - x_j(t)$. Subtracting (3.1) from (3.11), one gets

$$\begin{aligned} &\dot{e}_j - \frac{2}{q_j + q_{j+1}} ((\mathcal{T}_{j+1} - \tau_{j+1}) - (\mathcal{T}_j - \tau_j)) \\ &= -f(L) \left(\mathcal{N}(\xi_j) - \tau_{j+1/2}^\perp \right) - (f(L) - f(l_h)) \tau_{j+1/2}^\perp \\ &\quad + 2 \frac{(q_j - Q_j) + (q_{j+1} - Q_{j+1})}{(Q_j + Q_{j+1})(q_j + q_{j+1})} (\mathcal{T}_{j+1} - \mathcal{T}_j) + \mathcal{R}_j \\ &=: I_j^1 + I_j^2 + I_j^3 + I_j^4. \end{aligned}$$

Multiplying both sides with $\frac{1}{2}(q_j + q_{j+1})\dot{e}_j$ and summing together over all $j = 1, \dots, N$, we obtain

$$\frac{1}{2} \sum_{j=1}^N (q_j + q_{j+1}) |\dot{e}_j|^2 - \sum_{j=1}^N ((\mathcal{T}_{j+1} - \tau_{j+1}) - (\mathcal{T}_j - \tau_j)) \cdot \dot{e}_j = \sum_{k=1}^4 \sum_{j=1}^N \frac{1}{2} (q_j + q_{j+1}) I_j^k \cdot \dot{e}_j.$$

Applying (3.7), Young's inequality, Assumption 2.1 and (2.5a), we arrive at

$$\begin{aligned} & - \sum_{j=1}^N ((\mathcal{T}_{j+1} - \tau_{j+1}) - (\mathcal{T}_j - \tau_j)) \cdot \dot{e}_j \\ &= \frac{1}{2} \frac{d}{dt} \sum_{j=1}^N q_j |\mathcal{T}_j - \tau_j|^2 + h \sum_{j=1}^N \left(\frac{Q_j - q_j}{Q_j} \delta \dot{X}_j \cdot (\mathcal{T}_j - \tau_j) + \frac{q_j}{2Q_j} (\delta \dot{X}_j \cdot \mathcal{T}_j) |\mathcal{T}_j - \tau_j|^2 \right) \\ &\geq \frac{1}{2} \frac{d}{dt} \sum_{j=1}^N q_j |\mathcal{T}_j - \tau_j|^2 - C \sum_{j=1}^N \left(\frac{1}{h} (Q_j - q_j)^2 + q_j |\mathcal{T}_j - \tau_j|^2 \right), \end{aligned}$$

where for the first equality, we used the result in [15] (cf. page 9 in [15]). Employing (2.5d), (3.7), (3.8), (3.10) and Young's inequality, we get

$$\begin{aligned} \sum_{j=1}^N \frac{q_j + q_{j+1}}{2} I_j^1 \cdot \dot{e}_j &\leq Ch \sum_{j=1}^N |\mathcal{N}(\xi_j) - \tau_{j+1/2}^\perp| |\dot{e}_j| \\ &\leq C(\varepsilon) h \sum_{j=1}^N |\mathcal{T}_j - \tau_j|^2 + \varepsilon h \sum_{j=1}^N |\dot{e}_j|^2 + C(\varepsilon) h^4. \end{aligned}$$

Similarly, using (2.5a), (2.5c), Young's inequality and (3.13), one obtains

$$\begin{aligned} \sum_{j=1}^N \frac{1}{2} (q_j + q_{j+1}) I_j^3 \cdot \dot{e}_j &\leq C \sum_{j=1}^N (|Q_j - q_j| + |Q_{j+1} - q_{j+1}|) |\dot{e}_j| \\ &\leq \varepsilon h \sum_{j=1}^N |\dot{e}_j|^2 + \frac{C(\varepsilon)}{h} \sum_{j=1}^N |Q_j - q_j|^2, \\ \sum_{j=1}^N \frac{1}{2} (q_j + q_{j+1}) I_j^4 \cdot \dot{e}_j &\leq \varepsilon h \sum_{j=1}^N |\dot{e}_j|^2 + C(\varepsilon) h^4. \end{aligned}$$

It remains to estimate the term related to I_j^2 . Firstly we estimate the error of the

perimeter by applying the trapezoidal quadrature formula and (2.5a)

$$\begin{aligned}
|L - l_h| &= \left| \int_{\mathbb{S}^1} |\partial_\xi X| \, d\xi - \sum_{j=1}^N \frac{q_j + q_{j+1}}{2} \right| \\
&= \left| h \sum_{j=1}^N |\partial_\xi X|(\xi_j) + O(h^2) - \sum_{j=1}^N \frac{q_j + q_{j+1}}{2} \right| \\
&= \left| \sum_{j=1}^N \frac{Q_j + Q_{j+1}}{2} + O(h^2) - \sum_{j=1}^N \frac{q_j + q_{j+1}}{2} \right| \\
&\leq \sum_{j=1}^N |Q_j - q_j| + Ch^2.
\end{aligned} \tag{3.15}$$

This immediately yields

$$\begin{aligned}
\sum_{j=1}^N \frac{1}{2} (q_j + q_{j+1}) I_j^2 \cdot \dot{e}_j &\leq Ch \sum_{j=1}^N |L - l_h| |\dot{e}_j| \leq C(\varepsilon) |L - l_h|^2 + \varepsilon h \sum_{j=1}^N |\dot{e}_j|^2 \\
&\leq C(\varepsilon) \left(\sum_{j=1}^N |Q_j - q_j| \right)^2 + C(\varepsilon) h^4 + \varepsilon h \sum_{j=1}^N |\dot{e}_j|^2 \\
&\leq C(\varepsilon) \frac{1}{h} \sum_{j=1}^N |Q_j - q_j|^2 + C(\varepsilon) h^4 + \varepsilon h \sum_{j=1}^N |\dot{e}_j|^2.
\end{aligned}$$

By combining the above inequalities, (3.7) and choosing ε to be sufficiently small, we are led to

$$h \sum_{j=1}^N |\dot{e}_j|^2 + \frac{d}{dt} \sum_{j=1}^N q_j |\mathcal{T}_j - \tau_j|^2 \leq Ch^4 + C \sum_{j=1}^N \left(\frac{1}{h} (Q_j - q_j)^2 + q_j |\mathcal{T}_j - \tau_j|^2 \right).$$

Through integration and utilizing Gronwall's inequality, we obtain

$$\int_0^t h \sum_{j=1}^N |\dot{e}_j|^2 \, ds + \sup_{0 \leq s \leq t} \sum_{j=1}^N q_j |\mathcal{T}_j - \tau_j|^2 \leq Ch^4 + C \int_0^t \frac{1}{h} \sum_{j=1}^N (Q_j - q_j)^2 \, ds, \tag{3.16}$$

for $0 \leq t \leq T^*$, where C is a constant depending on $C_1, C_2, K_1(X), T$ and f .

(3). *Length difference estimate.* By using (3.9) and (3.15), we can derive the following estimates

$$(|\dot{x}_j|^2 - |\dot{X}_j|^2) \leq (|\dot{x}_j| + |\dot{X}_j|) |\dot{x}_j - \dot{X}_j| \leq C |\dot{e}_j|, \quad f(l_h) - f(L) \leq C \sum_{j=1}^N |Q_j - q_j| + Ch^2.$$

Subtracting (3.12) from (3.3), integrating from 0 to t , and applying (2.5d) together

with the above estimate, we get

$$\begin{aligned}
|Q_j - q_j|(t) &\leq \int_0^t |\dot{Q}_j - \dot{q}_j|(s) \, ds + |Q_j - q_j|(0) \\
&\leq C \int_0^t |q_j - Q_j| + |q_{j+1} - Q_{j+1}| + |q_{j-1} - Q_{j-1}| \, ds \\
&\quad + Ch \int_0^t |\tau_j - \mathcal{T}_j| + |\tau_{j+1} - \mathcal{T}_{j+1}| + |\tau_{j-1} - \mathcal{T}_{j-1}| \, ds \\
&\quad + Ch \int_0^t \sum_{j=1}^N |Q_j - q_j| \, ds + Ch^3 + Ch \int_0^t |\dot{e}_{j-1}| + |\dot{e}_j| \, ds + \int_0^t |\tilde{\mathcal{R}}_j| \, ds.
\end{aligned}$$

This together with (3.14) yields

$$\begin{aligned}
\frac{1}{h} \sum_{j=1}^N (Q_j - q_j)^2(t) &\leq C \int_0^t h \sum_{j=1}^N |\dot{e}_j|^2 \, ds + C \int_0^t \frac{1}{h} \sum_{j=1}^N (Q_j - q_j)^2 \, ds \\
&\quad + C \int_0^t h \sum_{j=1}^N |\mathcal{T}_j - \tau_j|^2 \, ds + Ch^4.
\end{aligned}$$

Applying Gronwall's inequality, we get

$$\begin{aligned}
\frac{1}{h} \sum_{j=1}^N (Q_j - q_j)^2(t) &\leq C \int_0^t h \sum_{j=1}^N |\dot{e}_j|^2 \, ds + C \int_0^t \sum_{j=1}^N q_j |\mathcal{T}_j - \tau_j|^2 \, ds + Ch^4 \\
&\leq C \int_0^t h \sum_{j=1}^N |\dot{e}_j|^2 \, ds + C \sup_{0 \leq s \leq t} \sum_{j=1}^N q_j |\mathcal{T}_j - \tau_j|^2 + Ch^4 \quad (3.17) \\
&\leq Ch^4 + C \int_0^t \frac{1}{h} \sum_{j=1}^N (Q_j - q_j)^2(s) \, ds,
\end{aligned}$$

where for the last inequality we utilized (3.16). Hence Gronwall's inequality gives

$$\frac{1}{h} \sum_{j=1}^N (Q_j - q_j)^2(t) \leq Ch^4, \quad 0 \leq t \leq T^*. \quad (3.18)$$

This together with (3.16) implies

$$\int_0^{T^*} h \sum_{j=1}^N |\dot{e}_j|^2 \, ds + \sup_{0 \leq t \leq T^*} \sum_{j=1}^N q_j |\mathcal{T}_j - \tau_j|^2 \leq Ch^4. \quad (3.19)$$

Now we are ready to complete the proof by a continuity argument. It follows from (3.19) that there exists $h_2 > 0$ such that when $h \leq h_2$,

$$|\mathcal{T}_j - \tau_j|(t) \leq h^{-\frac{1}{2}} \left(h \sum_{k=1}^N |\mathcal{T}_k - \tau_k|^2(t) \right)^{\frac{1}{2}} \leq Ch^{-\frac{1}{2}} h^2 \leq \frac{1}{2} h^{\frac{5}{4}}, \quad 0 \leq t \leq T^*.$$

On the other hand, it can be easily derived from (3.18) that

$$|Q_j(t) - q_j(t)| \leq Ch^{3/2}, \quad 0 \leq t \leq T^*,$$

which together with (2.5a) yields

$$\frac{2}{3}C_1 \leq q_j(t)/h \leq \frac{3}{2}C_2, \quad h \leq h_3.$$

By continuity we can extend T^* such that

$$\frac{C_1}{2} \leq \frac{q_j(t)}{h} \leq 2C_2, \quad \max_{j=1,\dots,N} |\mathcal{T}_j(t) - \tau_j(t)| \leq h^{\frac{5}{4}}.$$

This contradicts (3.7) if $T^* < T$. Therefore, $T^* = T$. As for the estimate of e_j , we first notice

$$\delta e_j = \delta X_j - \delta x_j = \frac{Q_j(\mathcal{T}_j - \tau_j)}{h} + \frac{(Q_j - q_j)}{h} \tau_j.$$

Recalling (3.18) and (3.19), we immediately get

$$\begin{aligned} h \sum_{j=1}^N |e_j|^2 &\leq C \int_0^t h \sum_{j=1}^N |\dot{e}_j|^2 ds \leq Ch^4, \\ h \sum_{j=1}^N |\delta e_j|^2 &\leq Ch \sum_{j=1}^N \left(|\mathcal{T}_j - \tau_j|^2 + \frac{(Q_j - q_j)^2}{h^2} \right) \leq Ch^4, \end{aligned}$$

which yields

$$\|X(t) - x_h(t)\|_{H_G^1} = \left(h \sum_{j=1}^N (|e_j|^2 + |\delta e_j|^2) \right)^{\frac{1}{2}} \leq Ch^2, \quad 0 \leq t \leq T,$$

and the proof is completed by taking $h_0 = \min\{h_1, h_2, h_3\}$. \square

4 Finite element methods

In this section, we present two finite element methods based on different formulations and establish their error estimates. The parametrization (1.2) naturally leads to a weak formulation: for any $v \in (H^1(\mathbb{S}^1))^2$, it holds

$$\int_{\mathbb{S}^1} |\partial_\xi X| \partial_t X \cdot v \, d\xi + \int_{\mathbb{S}^1} \mathcal{T} \cdot \partial_\xi v \, d\xi + \int_{\mathbb{S}^1} f(L)(\partial_\xi X)^\perp \cdot v \, d\xi = 0. \quad (4.1)$$

For spatial discretization, let $0 = \xi_0 < \xi_1 < \dots < \xi_N = 2\pi$ be a partition of \mathbb{S}^1 . We denote $h_j = \xi_j - \xi_{j-1}$ as the length of the interval $I_j := [\xi_{j-1}, \xi_j]$ and $h = \max_j h_j$. We assume that the partition and the exact solution are regular in the following senses, respectively:

(Assumption 4.1) There exist constants c_p and c_P such that

$$\min_j h_j \geq c_p h, \quad |h_{j+1} - h_j| \leq c_P h^2, \quad 1 \leq j \leq N.$$

(Assumption 4.2) Suppose the solution of (1.2) satisfies $X \in W^{1,\infty}([0, T], H^2(\mathbb{S}^1))$, i.e.,

$$K_2(X) := \|X\|_{W^{1,\infty}([0, T], H^2(\mathbb{S}^1))} < \infty,$$

and there exist constants $0 < C_1 < C_2$ such that (2.4) holds.

We define the following finite element space consisting of piecewise linear functions satisfying periodic boundary conditions:

$$V_h = \{v \in C(\mathbb{S}^1, \mathbb{R}^2) : v|_{I_j} \in P_1(I_j), \quad 1 \leq j \leq N, \quad v(\xi_0) = v(\xi_N)\},$$

where P_1 denotes all polynomials with degrees at most 1. For any continuous function $v \in C(\mathbb{S}^1, \mathbb{R}^2)$, the linear interpolation $I_h v \in V_h$ is uniquely determined through $I_h v(\xi_j) = v(\xi_j)$ for all $1 \leq j \leq N$ and can be explicitly written as $I_h v(\xi) = \sum_{j=1}^N v(\xi_j) \varphi_j(\xi)$, where φ_j represents the standard Lagrange basis function satisfying $\varphi_j(\xi_i) = \delta_{ij}$.

4.1 FEM with only the normal motion

In this part, we present a finite element method based on the original parametrization (1.2).

Definition 4.1 We call a function

$$x_h(\xi, t) = \sum_{j=1}^N x_j(t) \varphi_j(\xi) : \mathbb{S}^1 \times [0, T] \rightarrow \mathbb{R}^2 \quad (4.2)$$

is a semi-discrete solution of (1.2) if it satisfies $x_h(\xi, 0) = I_h X^0$ and for all $v_h \in V_h$, it holds

$$\int_{\mathbb{S}^1} q_h \partial_t x_h \cdot v_h \, d\xi + \int_{\mathbb{S}^1} \tau_h \cdot \partial_\xi v_h \, d\xi + \int_{\mathbb{S}^1} \frac{\mathbf{h}^2 q_h}{6} \partial_\xi \partial_t x_h \cdot \partial_\xi v_h \, d\xi + \int_{\mathbb{S}^1} f(l_h) (\partial_\xi x_h)^\perp \cdot v_h \, d\xi = 0, \quad (4.3)$$

where

$$q_h = |\partial_\xi x_h| = \sum_{j=1}^N \frac{q_j}{h_j} \chi_{I_j}, \quad \tau_h = \frac{\partial_\xi x_h}{|\partial_\xi x_h|} = \sum_{j=1}^N \frac{x_j - x_{j-1}}{q_j} \chi_{I_j}, \quad (4.4)$$

represent the discrete length element and unit tangent vector, respectively, l_h represents the perimeter of the evolved polygon with vertices x_j , and $\mathbf{h} = \sum_{j=1}^N h_j \chi_{I_j}$ with χ being the characteristic function.

Remark 4.2 Compared to the original formulation (4.1), here an extra term $\int_{\mathbb{S}^1} \frac{\mathbf{h}^2 |\partial_\xi x_h|}{6} \partial_\xi \partial_t x_h \cdot \partial_\xi v_h \, d\xi$ is introduced in (4.3), which reduces to the so-called mass-lumped scheme (4.5). Clearly this term does not affect the convergence order for a linear finite element method. As was interpreted in [26, 21], this mass-lumped version can preserve the length shortening property for the CSF/AP-CSF, which was missing for the original formula.

Taking $v_h = (\varphi_j, 0)$ and $v_h = (0, \varphi_j)$ for $j = 1, \dots, N$ in (4.3), we are led to the following $2N$ ordinary differential equations:

$$\frac{q_j + q_{j+1}}{2} \dot{x}_j = \tau_{j+1} - \tau_j - f(l_h)(x_{j+1} - x_{j-1})^\perp, \quad (4.5)$$

where τ_j is the discrete tangent defined as (2.3). Furthermore, we have the following identities

$$\dot{q}_j = -\frac{1}{q_j + q_{j+1}} |\tau_{j+1} - \tau_j|^2 - \frac{1}{q_j + q_{j-1}} |\tau_{j-1} - \tau_j|^2 + \tau_j \cdot (r_j - r_{j-1}) \quad (4.6)$$

$$= -\frac{q_j + q_{j+1}}{4} |\dot{x}_j - r_j|^2 - \frac{q_j + q_{j-1}}{4} |\dot{x}_{j-1} - r_{j-1}|^2 + \tau_j \cdot (r_j - r_{j-1}), \quad (4.7)$$

where for simplicity we denote

$$r_j = -f(l_h) \frac{n_j q_j + n_{j+1} q_{j+1}}{q_j + q_{j+1}}. \quad (4.8)$$

Theorem 4.3 *Let $X(\xi, t)$ be a solution of (1.2) satisfying Assumption 4.2. Assume that the partition of \mathbb{S}^1 satisfies Assumption 4.1. Then there exists $h_0 > 0$ such that for all $0 < h \leq h_0$, there exists a unique semi-discrete solution x_h for (4.3). Furthermore, the solution satisfies*

$$\int_0^T \|\partial_t X - \partial_t x_h\|_{L^2}^2 dt + \sup_{t \in [0, T]} \|X - x_h\|_{H^1}^2 \leq Ch^2, \quad (4.9)$$

where h_0 and C depend on $c_p, c_P, C_1, C_2, T, K_2(X)$ and f .

Before presenting the proof of Theorem 4.3, we first list a lemma which will be used later.

Lemma 4.4 [26, Lemma 4.2] *Under Assumptions 3.1 and 3.2, suppose further*

$$\int_{\mathbb{S}^1} |\mathcal{T} - \tau_h|^2 q_h d\xi + \|\partial_\xi X - q_h\|_{L^2}^2 \leq Ch^2, \quad \forall t \in [0, T^*],$$

then there exists a constant h_0 such that for any $0 < h \leq h_0$, we have

$$\inf_\xi q_h \geq 3C_1/4, \quad \text{and} \quad \sup_\xi q_h \leq 3C_2/2, \quad \forall t \in [0, T^*],$$

where C_1 and C_2 are the lower and upper bounds of $|\partial_\xi X|$ shown in (2.4).

Proof Similar to the proof of Theorem 3.2, we apply the continuity argument. Define

$$T^* = \sup\{t \in [0, T] : (4.3) \text{ has a unique solution } x_h \text{ and } \inf q_h \geq C_1/2, \sup q_h \leq 2C_2\}. \quad (4.10)$$

Since the nonlinear terms in (4.5) are locally Lipschitz with respect to x_j , the local existence and uniqueness follow from standard ODE theory, and thus $T^* > 0$. Moreover, due to the Lipschitz property of f and Assumption (4.10), for any $t \in [0, T^*]$, it holds that

$$2\pi C_1 \leq L \leq 2\pi C_2, \quad \pi C_1 \leq l_h \leq 4\pi C_2, \quad |f(L)| \leq C, \quad (4.11)$$

where C is a constant depending on C_1, C_2, f .

- (1) *Stability.* Taking the difference between (4.1) and (4.3), and choosing $v_h = I_h(\partial_t X) - \partial_t x_h \in V_h$, we get

$$\begin{aligned}
& \int_{\mathbb{S}^1} |\partial_t X - \partial_t x_h|^2 q_h d\xi + \int_{\mathbb{S}^1} (\mathcal{T} - \tau_h) (\partial_\xi \partial_t X - \partial_\xi \partial_t x_h) d\xi \\
&= \int_{\mathbb{S}^1} \partial_t X \cdot (q_h - |\partial_\xi X|) (I_h \partial_t X - \partial_t x_h) d\xi + \int_{\mathbb{S}^1} \frac{\mathbf{h}^2 q_h}{6} \partial_\xi \partial_t x_h \cdot \partial_\xi (I_h \partial_t X - \partial_t x_h) d\xi \\
&+ \int_{\mathbb{S}^1} q_h (\partial_t X - \partial_t x_h) \cdot (\partial_t X - I_h \partial_t X) d\xi + \int_{\mathbb{S}^1} (\mathcal{T} - \tau_h) \cdot (\partial_\xi \partial_t X - \partial_\xi I_h \partial_t X) d\xi \\
&+ \int_{\mathbb{S}^1} f(L) (\partial_\xi X - \partial_\xi x_h)^\perp \cdot (\partial_t x_h - I_h \partial_t X) d\xi \\
&+ \int_{\mathbb{S}^1} (f(L) - f(l_h)) (\partial_\xi x_h)^\perp \cdot (\partial_t x_h - I_h \partial_t X) d\xi =: J_1 + J_2 + J_3 + J_4 + J_5 + J_6.
\end{aligned}$$

The estimates of the second term on the left side and J_j for $1 \leq j \leq 4$ can be found in [21, Lemma 5.1] or [26, Lemma 4.1], which can be summarized as follows:

$$\begin{aligned}
& \int_{\mathbb{S}^1} (\mathcal{T} - \tau_h) \cdot (\partial_\xi \partial_t X - \partial_\xi \partial_t x_h) d\xi \\
&\geq \frac{1}{2} \frac{d}{dt} \left(\int_{\mathbb{S}^1} |\mathcal{T} - \tau_h|^2 q_h d\xi \right) - C \|\partial_\xi \partial_t X\|_{L^\infty} \left(\int_{\mathbb{S}^1} |\mathcal{T} - \tau_h|^2 q_h d\xi + \|\partial_\xi X - q_h\|_{L^2}^2 \right), \\
&J_1 + J_2 + J_3 + J_4 \leq \varepsilon \int_{\mathbb{S}^1} |\partial_t X - \partial_t x_h|^2 q_h d\xi + C(\varepsilon) \|\partial_t X\|_{L^\infty}^2 \|\partial_\xi X - q_h\|_{L^2}^2 \\
&\quad + C(\varepsilon) h^2 \|\partial_t X\|_{H^1}^2 + C \int_{\mathbb{S}^1} |\mathcal{T} - \tau_h|^2 q_h d\xi,
\end{aligned}$$

where ε is a generic positive constant which will be chosen later. For J_5 and J_6 , in view of the Lipschitz property of f , (4.11), and the identity

$$|\partial_\xi X - \partial_\xi x_h|^2 = (|\partial_\xi X| - q_h)^2 + |\partial_\xi X| q_h |\mathcal{T} - \tau_h|^2, \quad (4.12)$$

applying similar techniques in [26] (cf. proof of Lemma 4.1), we can get

$$\begin{aligned}
J_5 &= \int_{\mathbb{S}^1} f(L) (\partial_\xi X - \partial_\xi x_h)^\perp \cdot (\partial_t X - I_h \partial_t X) d\xi \\
&\quad + \int_{\mathbb{S}^1} f(L) (\partial_\xi X - \partial_\xi x_h)^\perp \cdot (\partial_t x_h - \partial_t X) d\xi \\
&\leq C \|\partial_\xi X\|_{L^\infty} \int_{\mathbb{S}^1} |\mathcal{T} - \tau_h|^2 q_h d\xi + C \int_{\mathbb{S}^1} (|\partial_\xi X| - q_h)^2 d\xi + C h^2 \|\partial_t X\|_{H^1}^2 \\
&\quad + C(\varepsilon) \|\partial_\xi X\|_{L^\infty} \int_{\mathbb{S}^1} |\mathcal{T} - \tau_h|^2 q_h d\xi + C(\varepsilon) \|\partial_\xi X - q_h\|_{L^2}^2 + \varepsilon \int_{\mathbb{S}^1} |\partial_t x_h - \partial_t X|^2 q_h d\xi, \\
J_6 &= \int_{\mathbb{S}^1} (f(L) - f(l_h)) (\partial_\xi x_h)^\perp \cdot (\partial_t X - I_h \partial_t X) d\xi \\
&\quad + \int_{\mathbb{S}^1} (f(L) - f(l_h)) (\partial_\xi x_h)^\perp \cdot (\partial_t x_h - \partial_t X) d\xi \\
&\leq C |L - l_h|^2 + C \|\partial_t X - I_h \partial_t X\|_{L^2}^2 + C(\varepsilon) |L - l_h|^2 + \varepsilon \int_{\mathbb{S}^1} q_h |\partial_t x_h - \partial_t X|^2 d\xi \\
&\leq C(\varepsilon) \|\partial_\xi X - q_h\|_{L^2}^2 + C h^2 \|\partial_t X\|_{H^1}^2 + \varepsilon \int_{\mathbb{S}^1} q_h |\partial_t x_h - \partial_t X|^2 d\xi.
\end{aligned}$$

Here we use the inequalities $|L - l_h|^2 \leq \| |\partial_\xi X| - q_h \|_{L^1}^2 \leq C \| |\partial_\xi X| - q_h \|_{L^2}^2$. Combining all the above estimates, we are led to

$$\begin{aligned} \int_{\mathbb{S}^1} |\partial_t X - \partial_t x_h|^2 q_h d\xi + \frac{1}{2} \frac{d}{dt} \int_{\mathbb{S}^1} |\mathcal{T} - \tau_h|^2 q_h d\xi &\leq 4\varepsilon \int_{\mathbb{S}^1} |\partial_t X - \partial_t x_h|^2 q_h d\xi \\ &+ C(\varepsilon) h^2 \| \partial_t X \|_{H^2}^2 + C(\varepsilon, K_2(X)) \| |\partial_\xi X| - q_h \|_{L^2}^2 + C(\varepsilon, K_2(X)) \int_{\mathbb{S}^1} |\mathcal{T} - \tau_h|^2 q_h d\xi. \end{aligned}$$

Choosing ε small enough, integrating both sides with respect to time from 0 to t and applying Gronwall's argument, we arrive at

$$\int_0^t \int_{\mathbb{S}^1} |\partial_t X - \partial_t x_h|^2 q_h d\xi ds + \sup_{0 \leq s \leq t} \int_{\mathbb{S}^1} |\mathcal{T} - \tau_h|^2 q_h d\xi \leq C \int_0^t \| |\partial_\xi X| - q_h \|_{L^2}^2 ds + Ch^2, \quad (4.13)$$

where C is a constant depending on $c_p, c_P, C_1, C_2, T, K_2(X)$ and f .

- (2) *Length difference estimate.* Applying the Lipschitz property of f and (4.11), a mild modification of the proof of [26, Lemma 4.3, Lemma 4.4] enables us to establish the same length difference estimate as in [26]:

$$\| |\partial_\xi X| - q_h \|_{L^2}^2 \leq C \int_0^t \int_{\mathbb{S}^1} |\partial_t X - \partial_t x_h|^2 q_h d\xi ds + C \int_0^t \int_{\mathbb{S}^1} |\mathcal{T} - \tau_h|^2 q_h d\xi ds + Ch^2, \quad (4.14)$$

where C depends on $c_p, c_P, C_1, C_2, T, K_2(X)$ and f . For the details, we refer to [26].

Combining (4.13) and (4.14), employing Gronwall's inequality, we derive

$$\int_0^t \int_{\mathbb{S}^1} |\partial_t X - \partial_t x_h|^2 q_h d\xi ds + \sup_{0 \leq s \leq t} \int_{\mathbb{S}^1} |\mathcal{T} - \tau_h|^2 q_h d\xi \leq Ch^2, \quad \forall t \in [0, T^*], \quad (4.15)$$

which together with (4.14) yields

$$\| |\partial_\xi X| - q_h \|_{L^2}^2 \leq Ch^2.$$

Applying Lemma 4.4, there exists $h_0 > 0$ depending on $c_p, c_P, C_1, C_2, T, K_2(X)$ such that for any $0 < h \leq h_0$, we have

$$\inf q_h \geq 3C_1/4, \quad \text{and} \quad \sup q_h \leq 3C_2/2, \quad t \in [0, T^*].$$

By standard ODE theory, we can uniquely extend the above semi-discrete solution in a neighborhood of T^* , and thus $T^* = T$. The estimate (4.9) can be concluded similarly as in [26, Theorem 2.5] by integration, (4.12) and (4.15):

$$\begin{aligned} \|X(\cdot, t) - x_h(\cdot, t)\|_{H^1}^2 &= \int_{\mathbb{S}^1} |X - x_h|^2 d\xi + \int_{\mathbb{S}^1} |\partial_\xi X - \partial_\xi x_h|^2 d\xi \\ &\leq 2 \int_{\mathbb{S}^1} \left(\int_0^t |\partial_t X - \partial_t x_h| ds \right)^2 d\xi + 2 \|X^0 - I_h X^0\|_{L^2}^2 + \| |\partial_\xi X| - q_h \|_{L^2}^2 + \int_{\mathbb{S}^1} |\mathcal{T} - \tau_h|^2 |\partial_\xi X| q_h d\xi \\ &\leq 2 \int_{\mathbb{S}^1} T \int_0^t |\partial_t X - \partial_t x_h|^2 ds d\xi + Ch^2 \leq Ch^2, \end{aligned}$$

and the proof is completed. \square

4.2 FEM with tangential motions

The aforementioned methods are developed based on the equation (1.1) and only normal motion is allowed. They might suffer from the fact that the mesh will have inhomogeneous properties during the evolution, for instance, some nodes may cluster and the mesh may become distorted. This will lead to instability and even the breakdown of the simulation. To address this challenge, various techniques have been proposed to improve the mesh quality for evolving various types of geometric flows in the literature, such as mesh redistribution [3], and the introduction of artificial tangential velocity [6, 20, 30, 37].

In this subsection, to achieve equipartition property for long-time evolution, we derive another formulation of (1.1) by introducing a tangential velocity. We consider the equation

$$\partial_t X = (\kappa - f(L))\mathcal{N} + \gamma(X)\mathcal{T},$$

where \mathcal{N}, \mathcal{T} are the unit normal vector and tangent vector respectively, and γ is the tangential velocity to be determined. It is important to note that the presence of tangential velocity has no impact on the shape of evolving curves [12, 22], and suitable choices of tangential velocity may help the redistribution of mesh points [31, 30, 37]. As mentioned in the introduction, inspired by the work of [12, 22] for curve shortening flow, we consider an explicit tangential velocity given by

$$\gamma(X) = \frac{\partial_\xi X \cdot \partial_{\xi\xi} X}{|\partial_\xi X|^3}.$$

More generally, for a fixed parameter $0 < \alpha \leq 1$, we consider a series of reparametrizations X_α which are determined by

$$\alpha \partial_t X_\alpha + (1 - \alpha)(\partial_t X_\alpha \cdot \mathcal{N})\mathcal{N} = \frac{\partial_{\xi\xi} X_\alpha}{|\partial_\xi X_\alpha|^2} - f(L)\mathcal{N}; \quad X_\alpha(\xi, 0) = X^0(\xi). \quad (4.16)$$

Below we provide three justifications for (4.16).

- (i) The solution X_α of the evolution equation (4.16) has the same shape as the standard parametrization equation (1.2) since they share the same normal velocity

$$\begin{aligned} \partial_t X_\alpha \cdot \mathcal{N} &= \alpha \partial_t X_\alpha \cdot \mathcal{N} + (1 - \alpha) \partial_t X_\alpha \cdot \mathcal{N} \\ &= \left(\frac{\partial_{\xi\xi} X_\alpha}{|\partial_\xi X_\alpha|^2} - \gamma(X_\alpha)\mathcal{T} - f(L)\mathcal{N} \right) \cdot \mathcal{N} \\ &= \left(\frac{1}{|\partial_\xi X_\alpha|} \partial_\xi \left(\frac{\partial_\xi X_\alpha}{|\partial_\xi X_\alpha|} \right) - f(L)\mathcal{N} \right) \cdot \mathcal{N} \\ &= \kappa - f(L), \end{aligned}$$

where we note that the curvature κ and perimeter L are geometric quantities independent of the parametrization.

- (ii) The evolution of (4.16) has asymptotic equidistribution property in a continuous level. More precisely, suppose X_α^e is the equilibrium of (4.16), i.e., $\partial_t X_\alpha^e = 0$, then formally

we have

$$\partial_\xi |\partial_\xi X_\alpha^e| = \partial_\xi X_\alpha^e \cdot \mathcal{T} = \left(\frac{\partial_{\xi\xi} X_\alpha^e}{|\partial_\xi X_\alpha^e|^2} - f(L)\mathcal{N} \right) \cdot |\partial_\xi X_\alpha^e|^2 \mathcal{T} = 0,$$

which means the equilibrium has constant arc-length. This leads us to expect that the corresponding numerical solution for (4.16) has equidistributed mesh points for long-time evolution.

- (iii) As explained in [22, Section 8], we can write the standard parametrization equation (1.2) as

$$\partial_t X = \Delta_{\Gamma[X]} X - f(L)\mathcal{N},$$

where $\Gamma[X]$ is the image of X and $\Delta_{\Gamma[X]}$ is the Laplace-Beltrami operator over the curve $\Gamma[X]$. The DeTurck's trick for operator $\Delta_{\Gamma[X]}$ maintains the normal term $f(L)\mathcal{N}$ unaffected and leads to (4.16). In this aspect, the nonlocal flows can be viewed as a natural generalization of [22, Section 8].

Next we present a finite element method for (4.16). For fixed α , multiplying $|\partial_\xi X|^2$ for both sides of (4.16) (below we omit the subscript α for simplicity), we obtain the following weak formulation: for any $v \in (H^1(\mathbb{S}^1))^2$, it holds

$$\int_{\mathbb{S}^1} |\partial_\xi X|^2 (\alpha \partial_t X + (1 - \alpha)(\partial_t X \cdot \mathcal{N})\mathcal{N}) \cdot v d\xi + \int_{\mathbb{S}^1} \partial_\xi X \cdot \partial_\xi v d\xi + \int_{\mathbb{S}^1} f(L) |\partial_\xi X|^2 \mathcal{N} \cdot v d\xi = 0. \quad (4.17)$$

We use the same spatial discretization for \mathbb{S}^1 as in the last subsection and assume it satisfies Assumption 4.1. We further assume the exact solution of (4.16) is regular in the following sense.

(Assumption 4.3) Suppose that the solution of (4.16) with an initial value $X^0 \in H^2(\mathbb{S}^1)$ satisfies $X \in W^{1,\infty}([0, T], H^2(\mathbb{S}^1))$, i.e.,

$$K_2(X) := \|X\|_{W^{1,\infty}([0, T], H^2(\mathbb{S}^1))} < \infty,$$

and there exist constants $0 < C_1 < C_2$ such that (2.4) holds.

Definition 4.5 We call a function $x_h(\xi, t) = \sum_{j=1}^N x_j(t) \varphi_j(\xi) : \mathbb{S}^1 \times [0, T] \rightarrow \mathbb{R}^2$ is a semi-discrete solution of (4.16) if it satisfies $x_h(\xi, 0) = I_h X^0$ and

$$\int_{\mathbb{S}^1} |\partial_\xi x_h|^2 (\alpha \partial_t x_h + (1 - \alpha)(\partial_t x_h \cdot n_h) n_h) \cdot v_h d\xi + \int_{\mathbb{S}^1} \partial_\xi x_h \cdot \partial_\xi v_h d\xi + \int_{\mathbb{S}^1} f(l_h) |\partial_\xi x_h|^2 n_h \cdot v_h d\xi = 0, \quad (4.18)$$

for any $v_h \in V_h$, where $n_h = \tau_h^\perp$ represents the piecewise unit normal vector.

Theorem 4.6 Let $X(\xi, t)$ be a solution of (4.16) satisfying Assumption 4.3. Assume that the partition of \mathbb{S}^1 satisfies Assumption 4.1. Then there exists $h_0 > 0$ such that for all

$0 < h \leq h_0$, there exists a unique semi-discrete solution x_h for (4.18). Furthermore, the solution satisfies

$$\begin{aligned} \sup_{t \in [0, T]} |X - x_h|_{H^1}^2 + \alpha \int_0^T \|\partial_t X - \partial_t x_h\|_{L^2}^2 dt + (1 - \alpha) \int_0^T \|n_h \cdot (\partial_t X - \partial_t x_h)\|_{L^2}^2 dt \\ \leq CTh^2 + Ce^{MT/\alpha} h^2, \end{aligned}$$

where h_0 , C and M depend on c_p , c_P , C_1 , C_2 , $K_2(X)$, and f .

Proof Fix $\alpha \in (0, 1]$. We consider a Banach space $Z_h = C([0, T], V_h)$ equipped with the norm

$$\|v_h\|_{Z_h} := \sup_{t \in [0, T]} \|v_h(t)\|_{L^2}, \quad v_h \in Z_h,$$

and a nonempty closed convex subset B_h of Z_h defined by

$$B_h := \left\{ v_h \in Z_h \mid \sup_{t \in [0, T]} e^{-Mt/\alpha} \|(\partial_\xi X - \partial_\xi v_h)(t)\|_{L^2}^2 \leq K^2 h^2 \text{ and } v_h(\cdot, 0) = I_h X^0(\cdot) \right\}, \quad (4.19)$$

where $M, K > 0$ are constants that will be determined later. For any $u_h \in B_h$, applying interpolation error, inverse inequality and (4.19), one can easily derive

$$\begin{aligned} \|(\partial_\xi X - \partial_\xi u_h)(t)\|_{L^\infty} &\leq \|(\partial_\xi X - I_h \partial_\xi X)(t)\|_{L^\infty} + \|(I_h \partial_\xi X - \partial_\xi I_h u_h)(t)\|_{L^\infty} \\ &\leq Ch^{1/2} + Ch^{-1/2} \|(I_h \partial_\xi X - \partial_\xi u_h)(t)\|_{L^2} \\ &\leq Ch^{1/2} + Ch^{-1/2} (\|(\partial_\xi X - I_h \partial_\xi X)(t)\|_{L^2} + \|(\partial_\xi X - \partial_\xi u_h)(t)\|_{L^2}) \\ &\leq Ch^{1/2} \left(1 + e^{\frac{Mt}{2\alpha}} K \right). \end{aligned}$$

It follows from Assumption 4.3 that there exists a constant $h_0 > 0$ depending on $\alpha, M, K, T, K_2(X)$ such that for any $0 < h \leq h_0$, we have

$$\inf_{\xi} |\partial_\xi u_h| \geq C_1/2, \quad \sup_{\xi} |\partial_\xi u_h| \leq 2C_2. \quad (4.20)$$

Setting $\widehat{q}_h = |\partial_\xi u_h|$ and denoting \widehat{l}_h as the perimeter of u_h , due to the Lipschitz property of f , it holds that

$$2\pi C_1 \leq L \leq 2\pi C_2, \quad \pi C_1 \leq \widehat{l}_h \leq 4\pi C_2, \quad |f(\widehat{l}_h)| \leq C, \quad (4.21)$$

where C is a constant depending on C_1, C_2 and f . We define a continuous map $F : B_h \rightarrow Z_h$ as follows. For any $u_h \in B_h$, we define y_h as the unique solution of the following linear equation:

$$\begin{aligned} \int_{\mathbb{S}^1} \widehat{q}_h^2 (\alpha \partial_t y_h + (1 - \alpha) (\partial_t y_h \cdot \widehat{n}_h) \widehat{n}_h) \cdot v_h d\xi + \int_{\mathbb{S}^1} \partial_\xi y_h \cdot \partial_\xi v_h d\xi \\ + \int_{\mathbb{S}^1} f(\widehat{l}_h) \widehat{q}_h (\partial_\xi y_h)^\perp \cdot v_h d\xi = 0, \quad \forall v_h \in V_h, \end{aligned} \quad (4.22)$$

with initial data $y_h(0) = I_h X^0$, where $\widehat{n}_h = \left(\frac{\partial_\xi u_h}{|\partial_\xi u_h|} \right)^\perp$.

- (1) *Length difference estimate for $u_h \in B_h$.* Applying (4.19) and the triangle inequality, we obtain

$$\|(|\partial_\xi X| - \widehat{q}_h)(t)\|_{L^2} \leq \|(\partial_\xi X - \partial_\xi u_h)(t)\|_{L^2} \leq K h e^{Mt/(2\alpha)}, \quad 0 \leq t \leq T. \quad (4.23)$$

- (2) *Stability estimate for $y_h \in Z_h$.* Taking $v = v_h$ in (4.17) and subtracting (4.22) from (4.17), we get

$$\begin{aligned} & \int_{\mathbb{S}^1} \widehat{q}_h^2 (\alpha (\partial_t X - \partial_t y_h) \cdot v_h + (1 - \alpha) (\partial_t X - \partial_t y_h) \cdot \widehat{n}_h (\widehat{n}_h \cdot v_h)) \, d\xi \\ & \quad + \int_{\mathbb{S}^1} (\partial_\xi X - \partial_\xi y_h) \cdot \partial_\xi v_h \, d\xi \\ &= \int_{\mathbb{S}^1} (\widehat{q}_h^2 - |\partial_\xi X|^2) (\alpha \partial_t X \cdot v_h + (1 - \alpha) (\partial_t X \cdot \widehat{n}_h) (\widehat{n}_h \cdot v_h)) \, d\xi \\ & \quad + (1 - \alpha) \int_{\mathbb{S}^1} |\partial_\xi X|^2 (\partial_t X \cdot (\widehat{n}_h - \mathcal{N}) (\widehat{n}_h \cdot v_h) + (\partial_t X \cdot \mathcal{N}) (\widehat{n}_h - \mathcal{N}) \cdot v_h) \, d\xi \\ & \quad + \int_{\mathbb{S}^1} \left(-f(L) |\partial_\xi X| + f(\widehat{l}_h) \widehat{q}_h \right) (\partial_\xi X)^\perp \cdot v_h \, d\xi \\ & \quad - \int_{\mathbb{S}^1} f(\widehat{l}_h) \widehat{q}_h \left((\partial_\xi X)^\perp - (\partial_\xi y_h)^\perp \right) \cdot v_h \, d\xi =: J_1 + J_2 + J_3 + J_4. \end{aligned}$$

Choosing $v_h = I_h(\partial_t X) - \partial_t y_h \in V_h$, the estimates of the left-hand side and J_1, J_2 can be found in [22, (3.7)], which can be summarized as

$$\begin{aligned} & \frac{d}{dt} \|\partial_\xi X - \partial_\xi y_h\|_{L^2}^2 + \frac{C_1^2}{8} \alpha \|\partial_t X - \partial_t y_h\|_{L^2}^2 + \frac{C_1^2}{4} (1 - \alpha) \|\widehat{n}_h \cdot (\partial_t X - \partial_t y_h)\|_{L^2}^2 \\ & \leq C h^2 (1 + \|\partial_t X\|_{H^2}^2) + \|\partial_\xi X - \partial_\xi y_h\|_{L^2}^2 + C h^2 K^2 e^{Mt/\alpha} / \alpha + 2|J_3| + 2|J_4|. \end{aligned} \quad (4.24)$$

For the terms of J_3 and J_4 , in view of the Lipschitz property of f and the inequality

$$|L - \widehat{l}_h| \leq C \| |\partial_\xi X| - \widehat{q}_h \|_{L^2},$$

applying (4.20), (4.21), (4.23) and Young's inequality, we get

$$\begin{aligned} |J_3| &= \left| \int_{\mathbb{S}^1} \left(-f(L) + f(\widehat{l}_h) \right) |\partial_\xi X| (\partial_\xi X)^\perp \cdot v_h \, d\xi - \int_{\mathbb{S}^1} f(\widehat{l}_h) (|\partial_\xi X| - \widehat{q}_h) (\partial_\xi X)^\perp \cdot v_h \, d\xi \right| \\ &\leq C \int_{\mathbb{S}^1} |L - \widehat{l}_h| (|I_h(\partial_t X) - \partial_t X| + |\partial_t X - \partial_t y_h|) \, d\xi \\ &\quad + C \int_{\mathbb{S}^1} \| |\partial_\xi X| - \widehat{q}_h \| (|I_h(\partial_t X) - \partial_t X| + |\partial_t X - \partial_t y_h|) \, d\xi \\ &\leq C h |L - \widehat{l}_h| \|\partial_t X\|_{H^1} + C |L - \widehat{l}_h| \|\partial_t X - \partial_t y_h\|_{L^2} \\ &\quad + C h \| |\partial_\xi X| - \widehat{q}_h \|_{L^2} \|\partial_t X\|_{H^1} + C \| |\partial_\xi X| - \widehat{q}_h \|_{L^2} \|\partial_t X - \partial_t y_h\|_{L^2} \\ &\leq C K e^{\frac{Mt}{2\alpha}} h \|\partial_t X - \partial_t y_h\|_{L^2} + C K e^{\frac{Mt}{2\alpha}} h^2 \|\partial_t X\|_{H^1} \\ &\leq \frac{C(\varepsilon) e^{Mt/\alpha} K^2 h^2}{4\alpha} + \varepsilon \alpha \|\partial_t X - \partial_t y_h\|_{L^2}^2 + \alpha h^2 \|\partial_t X\|_{H^1}^2, \end{aligned}$$

and

$$\begin{aligned}
|J_4| &= \left| \int_{\mathbb{S}^1} f(\widehat{l}_h) \widehat{q}_h \left((\partial_\xi X)^\perp - (\partial_\xi y_h)^\perp \right) \cdot v_h \, d\xi \right| \\
&\leq Ch \|\partial_\xi X - \partial_\xi y_h\|_{L^2} \|\partial_t X\|_{H^1} + C \|\partial_\xi X - \partial_\xi y_h\|_{L^2} \|\partial_t X - \partial_t y_h\|_{L^2} \\
&\leq \|\partial_\xi X - \partial_\xi y_h\|_{L^2}^2 + Ch^2 \|\partial_t X\|_{H^1}^2 + \frac{C(\varepsilon)}{4\alpha} \|\partial_\xi X - \partial_\xi y_h\|_{L^2}^2 + \varepsilon \alpha \|\partial_t X - \partial_t y_h\|_{L^2}^2.
\end{aligned}$$

Combining all the above estimate and taking ε small enough, we obtain

$$\begin{aligned}
&\frac{d}{dt} \|\partial_\xi X - \partial_\xi y_h\|_{L^2}^2 + \frac{C_1^2}{16} \alpha \|\partial_t X - \partial_t y_h\|_{L^2}^2 + \frac{C_1^2}{4} (1 - \alpha) \|\widehat{n}_h \cdot (\partial_t X - \partial_t y_h)\|_{L^2}^2 \\
&\leq Ch^2 + C(1 + 1/\alpha) \|\partial_\xi X - \partial_\xi y_h\|_{L^2}^2 + Ch^2 K^2 e^{Mt/\alpha} / \alpha,
\end{aligned} \tag{4.25}$$

where C depends on c_p , c_P , C_1 , C_2 , T , $K_2(X)$, and f . This directly gives

$$\frac{d}{dt} \|\partial_\xi X - \partial_\xi y_h\|_{L^2}^2 \leq Ch^2 + C(1 + 1/\alpha) \|\partial_\xi X - \partial_\xi y_h\|_{L^2}^2 + Ch^2 K^2 e^{Mt/\alpha} / \alpha.$$

Thus we get

$$\begin{aligned}
&\|\partial_\xi X(t) - \partial_\xi y_h(t)\|_{L^2}^2 \\
&\leq \|\partial_\xi X^0 - \partial_\xi y_h(0)\|_{L^2}^2 e^{C(1+\frac{1}{\alpha})t} + Ch^2 \int_0^t e^{C(1+\frac{1}{\alpha})(t-s)} \left(1 + K^2 e^{Ms/\alpha} / \alpha \right) ds \\
&\leq C e^{C(1+\frac{1}{\alpha})t} h^2 + CK^2 h^2 \frac{e^{\frac{M}{\alpha}t} - e^{C(1+\frac{1}{\alpha})t}}{M - C(1 + \alpha)},
\end{aligned}$$

which yields

$$e^{-Mt/\alpha} \|\partial_\xi X - \partial_\xi y_h\|_{L^2}^2 \leq Ch^2 e^{(-\frac{M}{\alpha} + \frac{C}{\alpha} + C)t} + \frac{CK^2 h^2}{M - C(1 + \alpha)} \leq K^2 h^2, \tag{4.26}$$

if we select $M \geq 3C + C\alpha$ and $K^2 \geq 2C$. Hence, by plugging (4.26) into (4.25), integrating from 0 to T , we arrive at

$$\begin{aligned}
&\max_{t \in [0, T]} \|\partial_\xi X - \partial_\xi y_h\|_{L^2}^2 + \alpha \int_0^T \|\partial_t X - \partial_t y_h\|_{L^2}^2 \, dt + (1 - \alpha) \int_0^T \|\widehat{n}_h \cdot (\partial_t X - \partial_t y_h)\|_{L^2}^2 \, dt \\
&\leq C(1 + T)h^2 + CK^2 h^2 (1 + 1/\alpha) \int_0^T e^{Ms/\alpha} \, ds \\
&\leq C(1 + T)h^2 + K^2 h^2 (e^{MT/\alpha} - 1) \leq CT h^2 + C e^{MT/\alpha} h^2,
\end{aligned} \tag{4.27}$$

where C and M are constants depending on $c_p, c_P, K_2(X)$, C_1, C_2 and f .

Now we complete the proof by applying Schauder's fixed point theorem for F . Indeed, it follows from assumption (4.19) and (4.26) that $F(B_h) \subset B_h$. Furthermore, it can be easily derived from (4.27) and the assumption $y_h(0) = I_h X^0$ that $\|y_h\|_{W^{1,2}([0, T], V_h)} \leq C$, which, together with the Sobolev embedding, implies that the inclusion $F(B_h) \subset B_h$ is compact.

Thus, by Schauder's fixed point theorem (c.f. [22, Theorem 3.1]), there exists a fixed point x_h for (4.22) that satisfies $F(x_h) = x_h$, which is the desired semi-discrete solution. Moreover, the estimate (4.27) also holds for the solution x_h .

To address the uniqueness, it is important to recognize that (4.18) constitutes a nonlinear ODE system for x_j . Consequently, the uniqueness of x_h is assured by nonlinear ODE theory. It's evident that x_h serves as a semi-discrete solution of (4.18) and thus aligns with the corresponding estimate. \square

5 Convergence under manifold distance

As discussed in [42, 27], for two closed simple curves Γ_1 and Γ_2 , the manifold distance is defined as:

$$M(\Gamma_1, \Gamma_2) := \text{Area}((\Omega_1 \setminus \Omega_2) \cup (\Omega_2 \setminus \Omega_1)) = \text{Area}(\Omega_1) + \text{Area}(\Omega_2) - 2\text{Area}(\Omega_1 \cap \Omega_2),$$

where Ω_1 and Ω_2 are the regions enclosed by Γ_1 and Γ_2 respectively. As proved in [42, Proposition 5.1], the manifold distance satisfies symmetry, positivity and the triangle inequality. Under some assumptions, e.g., If Γ_2 lies within the tubular neighborhood of the C^2 curve Γ_1 [13], the manifold distance between the two curves can be interpreted as the L^1 -norm of the distance function. Recently, compare to the L^p -norm of parametrization functions, this type of distance (i.e. the L^p -norm of distance function) has gained wide attentions in both the scientific computing [27, 28] and numerical analysis community [1]. Moreover, the authors' works [42, 27, 28] have demonstrated that the manifold distance (one of the shape metrics) is more suitable than the norm of parametrization functions for quantifying numerical errors of the schemes which are used for solving geometric flows, especially for schemes which allow intrinsic tangential velocity. Meanwhile, Bai and Li [1] have recently observed that the L^2 -norm of distance function (so-called the projected distance in their paper) leads to the recovery of full H^1 parabolicity, and established a convergence result for Dziuk's scheme of the mean curvature flow with finite elements of degree $k \geq 3$.

In this subsection, we first show that the function L^∞ -norm is stronger than the manifold distance under some suitable regularity assumptions. More specifically, for a parametrization function $X \in C^2(\mathbb{S}^1)$ of curve Γ_X and an approximation curve Γ_Y by parameterization function $Y \in C^0(\mathbb{S}^1)$, we have the following lemma.

Lemma 5.1 *Let $X : \mathbb{S}^1 \rightarrow \mathbb{R}^2$ be a parametrization function of simple curves Γ_X with $X \in C^2(\mathbb{S}^1)$, and assume there exist constants $0 < C_1 < C_2$ such that (2.4) holds. Then there exist positive constants δ_0 and C such that for any parametrization function $Y \in C^0(\mathbb{S}^1)$ satisfying*

$$\|X - Y\|_{L^\infty} \leq \delta_0,$$

the following inequality holds:

$$M(\Gamma_X, \Gamma_Y) \leq C\|X - Y\|_{L^\infty},$$

where Γ_X and Γ_Y are the images of X and Y , respectively. The constants δ_0 and C depend on X , C_1 and C_2 .

Proof The closed simple C^2 curve Γ_X in \mathbb{R}^2 naturally admits a tabular neighborhood Ω_δ in the following manner [2, 13]: there exists a constant $\delta > 0$ such that the mapping

$$E_X : \Gamma_X \times (-\delta, \delta) \rightarrow \mathbb{R}^2, \quad E_X(a, \eta) = a + \eta \mathcal{N},$$

acts as a diffeomorphism from $\Gamma_X \times (-\delta, \delta)$ to the image denoted by $\text{Im}(E_X) =: \Omega_\delta$. Here \mathcal{N} represents the normal vector along Γ_X . Consequently, the points within the tabular neighborhood Ω_δ can be represented as

$$E_X^{-1} : \Omega_\delta \rightarrow \Gamma_X \times (-\delta, \delta), \quad E_X^{-1}(b) = (\pi_{\Gamma_X}(b), d_{\Gamma_X}(b)),$$

where $\pi_{\Gamma_X}(b) \in \Gamma_X$ is the projection of b onto Γ_X , and $d_{\Gamma_X}(b) = d(b, \Gamma_X)$ represents the signed distance.

Set $\delta_0 < \delta$. For any parametrization function $Y \in C^0(\mathbb{S}^1)$ which satisfies $\|X - Y\|_{L^\infty} \leq \delta_0$, it is evident that $\Gamma_Y \subseteq \Omega_\delta$. Now define

$$\delta_w := \sup_{b \in \Gamma_Y} |d_{\Gamma_X}(b)|$$

which represents the maximum distance between Γ_Y and Γ_X . Clearly, we can assume $\delta_w > 0$, as there is nothing to prove otherwise. Define two curves $\Gamma_{\delta_w}^{\text{int}}$ and $\Gamma_{\delta_w}^{\text{ext}}$, within the tabular neighborhood Ω_δ , which are parametrized as

$$\begin{aligned} \mathbb{S}^1 \ni \xi \rightarrow (x_{\text{int}}(\xi), y_{\text{int}}(\xi)) &= (x(\xi), y(\xi)) - \delta_w \mathcal{N}(x(\xi), y(\xi)), \\ \mathbb{S}^1 \ni \xi \rightarrow (x_{\text{ext}}(\xi), y_{\text{ext}}(\xi)) &= (x(\xi), y(\xi)) + \delta_w \mathcal{N}(x(\xi), y(\xi)), \end{aligned} \quad (5.1)$$

respectively. Here $X(\xi) = (x(\xi), y(\xi))$ is a parametrization of the curve Γ_X , and \mathcal{N} is the corresponding unit normal vector. Denote Ω_{δ_w} as the region enclosed by $\Gamma_{\delta_w}^{\text{int}}$ and $\Gamma_{\delta_w}^{\text{ext}}$ (cf. Fig 1 (a)). By utilizing the regularity assumption of X along with (2.4) and (5.1), we can

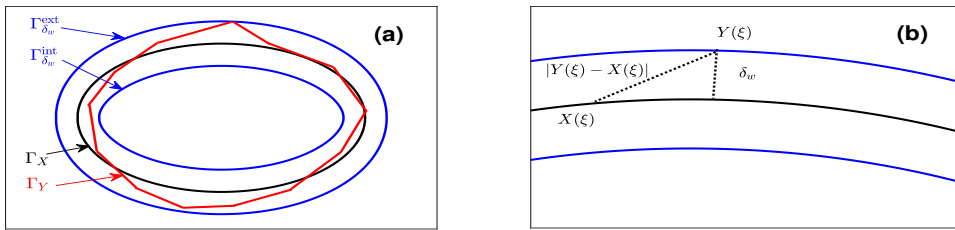


Figure 1: Illustration of (a) the definition of $\Gamma_X, \Gamma_Y, \Gamma_{\delta_w}^{\text{int}}$ and $\Gamma_{\delta_w}^{\text{ext}}$, (b) the comparison of the projection distance δ_w and the function L^∞ -norm $\|X - Y\|_{L^\infty}$.

estimate the area of Ω_{δ_w} as follows:

$$\begin{aligned} \text{Area}(\Omega_{\delta_w}) &= \int_{\mathbb{S}^1} \partial_\xi x_{\text{ext}} \cdot y_{\text{ext}} \, d\xi - \int_{\mathbb{S}^1} \partial_\xi x_{\text{int}} \cdot y_{\text{int}} \, d\xi \\ &\leq C \int_{\mathbb{S}^1} |\partial_\xi x_{\text{ext}} - \partial_\xi x_{\text{int}}| + |y_{\text{ext}} - y_{\text{int}}| \, d\xi \\ &\leq C\delta_w \int_{\mathbb{S}^1} |\partial_\xi \mathcal{N}| + |\mathcal{N}| \, d\xi \leq C\delta_w, \end{aligned}$$

where C is a constant depending on X, C_1 and C_2 . The triangle inequality for manifold distance yields

$$M(\Gamma_X, \Gamma_Y) \leq M(\Gamma_X, \Gamma_{\delta_w}^{\text{int}}) + M(\Gamma_{\delta_w}^{\text{int}}, \Gamma_Y) \leq 2\text{Area}(\Omega_{\delta_w}) \leq C\delta_w \leq C\|X - Y\|_{L^\infty},$$

where we use the natural control $\delta_w \leq \|X - Y\|_{L^\infty}$ (cf. Fig 1 (b)) and the proof is completed. \square

As natural corollaries, we have following convergence results of numerical schemes under the manifold distance.

Corollary 5.2 *We have the following convergence results under the manifold distance.*

- (1) *Let $X(\xi, t)$ be the solution of (1.2) satisfying Assumption 2.1 and $X \in W^{3,2}(\mathbb{S}^1)$. Let $x_h(t)$ be the unique finite difference semi-discrete solution of (3.1). Then we have*

$$\sup_{t \in [0, T]} M(\Gamma_X, \Gamma_{x_h}) \leq Ch^2.$$

- (2) *Let $X(\xi, t)$ be the solution of (1.2) satisfying Assumption 4.2 and $X \in W^{3,2}(\mathbb{S}^1)$. Assume that the partition of \mathbb{S}^1 satisfies Assumption 4.1 and $x_h(t)$ is the unique finite element semi-discrete solution of (4.3). Then we have*

$$\sup_{t \in [0, T]} M(\Gamma_X, \Gamma_{x_h}) \leq Ch.$$

- (3) *Let $X(\xi, t)$ be the solution of (4.16) satisfying Assumption 4.3 and $X \in W^{3,2}(\mathbb{S}^1)$. Assume that the partition of \mathbb{S}^1 satisfies Assumption 4.1 and $x_h(t)$ is the unique finite element semi-discrete solution of (4.18). Then we have*

$$\sup_{t \in [0, T]} M(\Gamma_X, \Gamma_{x_h}) \leq Ch.$$

For all the estimates, Γ_X and Γ_{x_h} represent the images of X and x_h , respectively, and the constant C depends on C_1, C_2, T, f and additionally, $K_1(X)$ for (1) and $K_2(X)$ for (2) and (3).

Proof For the first conclusion, combining the Sobolev embedding, triangle inequality, interpolation error, Lemma 5.3 with the main error estimate (3.2), one obtains

$$\begin{aligned} \|X - x_h\|_{L^\infty} &\leq C\|X - x_h\|_{H^1} \leq C\|X - I_h X\|_{H^1} + C\|I_h X - x_h\|_{H^1} \\ &\leq Ch^2\|X\|_{W^{3,2}} + C\|I_h X - x_h\|_{H_G^1} \sqrt{1 + h^2/6} \leq Ch^2, \end{aligned}$$

where for the third inequality we have utilized Lemma 5.3 for the grid function $I_h X - x_h$. Hence, by applying Lemma 5.1 with $\delta_0 = Ch^2$, $Y = x_h$ and for different time $t \in [0, T]$, we conclude the first assertion (1). The latter two statements can be similarly confirmed by referring to Theorems 4.3 and 4.6, along with the Sobolev embedding

$$\sup_{t \in [0, T]} \|X - x_h\|_{L^\infty} \leq C \sup_{t \in [0, T]} \|X - x_h\|_{H^1} \leq Ch,$$

and the proof is completed. \square

Lemma 5.3 *Let $g : \mathcal{G}_h \rightarrow \mathbb{R}$ be a grid function. Then we have*

$$\|g\|_{H^1}^2 \leq \|g\|_{H_G^1}^2 (1 + h^2/6),$$

where we identify a grid function g with the piecewise linear function over \mathbb{S}^1 that connects the grid values of g .

Proof Denote $M_j = \max_{\xi \in (\xi_j, \xi_{j+1})} (|g|^2)''$ and by applying the trapezoidal rule, we have

$$\begin{aligned} \|g\|_{H^1}^2 &= \sum_{j=1}^N \int_{\xi_j}^{\xi_{j+1}} |g|^2 + |\partial_\xi g|^2 \, d\xi \\ &\leq \sum_{j=1}^N \left(\frac{|g(\xi_j)|^2 + |g(\xi_{j+1})|^2}{2} h + \frac{h^3}{12} M_j \right) + h \sum_{j=1}^N |\delta g_j|^2 \\ &= h \sum_{j=1}^N (|g_j|^2 + |\delta g_j|^2) + \frac{h^3}{12} \sum_{j=1}^N M_j. \end{aligned}$$

Noticing g is a piecewise linear function, we have

$$M_j = \max_{\xi \in (\xi_j, \xi_{j+1})} (|g|^2)'' = 2 \max_{\xi \in (\xi_j, \xi_{j+1})} |g'|^2 = 2|\delta g_{j+1}|^2,$$

which yields

$$\|g\|_{H^1}^2 \leq h \sum_{j=1}^N (|g_j|^2 + |\delta g_j|^2) + \frac{h^3}{6} \sum_{j=1}^N |\delta g_{j+1}|^2 \leq \|g\|_{H_G^1}^2 \left(1 + \frac{1}{6} h^2 \right),$$

and the proof is completed. \square

6 Numerical results

In this section, we present numerous numerical experiments for the proposed three different schemes applied to various geometric flows involving the nonlocal term $f(L)$. We first provide full discretizations for the three schemes using backward Euler time discretization. Specifically, we choose an integer m , set the time step $\tau = T/m$ and $t_k = k\tau$ for $k = 0, \dots, m$. Given a fixed mesh size h and a time step $\tau = O(h^2)$, we consider the following three cases.

- (i) For the finite difference method (3.1), given $x_h^0 = I_h X^0$, for $k \geq 1$, we consider the solution $x_h^k \in \mathcal{G}_h$ of the following equation (**denoted as FDM**)

$$\frac{x_j^k - x_j^{k-1}}{\tau} = \frac{2}{q_j^{k-1} + q_{j+1}^{k-1}} \left(\frac{x_{j+1}^k - x_j^k}{q_{j+1}^{k-1}} - \frac{x_j^k - x_{j-1}^k}{q_j^{k-1}} \right) - f(l_h^{k-1}) \frac{n_j^{k-1} + n_{j+1}^{k-1}}{|n_j^{k-1} + n_{j+1}^{k-1}|}, \quad (6.1)$$

where x_j^k represents the grid value, l_h^k is the perimeter of the polygon with vertices $\{x_j^k\}_j$, and $n_j^k = (\tau_j^k)^\perp$ is the discrete normal vector.

- (ii) For the finite element method (4.3), given $x_h^0 = I_h X^0$, for $k \geq 1$, we consider the solution $x_h^k = \sum_{j=1}^N x_j^k \varphi_j \in V_h$ which satisfies (**denoted as FEM**)

$$\begin{aligned} & \int_{\mathbb{S}^1} \left| \partial_\xi x_h^{k-1} \right| \delta_\tau x_h^k \cdot v_h d\xi + \int_{\mathbb{S}^1} \partial_\xi x_h^k \cdot \partial_\xi v_h / \left| \partial_\xi x_h^{k-1} \right| d\xi \\ & + \int_{\mathbb{S}^1} \mathbf{h}^2 |\partial_\xi x_h^{k-1}| \partial_\xi \delta_\tau x_h^k \cdot \partial_\xi v_h / 6 d\xi + \int_{\mathbb{S}^1} f(l_h^{k-1}) (\partial_\xi x_h^k)^\perp \cdot v_h d\xi = 0, \quad \forall v_h \in V_h, \end{aligned}$$

where δ_τ is the backward finite difference $\delta_\tau x_h^k = (x_h^k - x_h^{k-1})/\tau$, and l_h^{k-1} is the length of the image of x_h^{k-1} . Or it can be written equivalently as a discretization for the ODE system (4.5):

$$\frac{q_j^{k-1} + q_{j+1}^{k-1}}{2\tau} (x_j^k - x_j^{k-1}) - \frac{x_{j+1}^k - x_j^k}{q_{j+1}^{k-1}} + \frac{x_j^k - x_{j-1}^k}{q_j^{k-1}} + \frac{f(l_h^{k-1})}{2} (x_{j+1}^k - x_{j-1}^k)^\perp = 0. \quad (6.2)$$

- (iii) For the finite element method with tangent motions (4.18), given $x_h^0 = I_h X^0$, for fixed $\alpha \in (0, 1]$ and $k \geq 1$, $x_h^k = \sum_{j=1}^N x_j^k \varphi_j \in V_h$ is the solution of the following (**denoted as FEM-TM**)

$$\begin{aligned} & \int_{\mathbb{S}^1} I_h \left[(\alpha \cdot \delta_\tau x_h^k + (1 - \alpha) \cdot (\delta_\tau x_h^k \cdot n_h^{k-1}) n_h^{k-1}) \cdot v_h \right] |\partial_\xi x_h^{k-1}|^2 d\xi + \int_{\mathbb{S}^1} \partial_\xi x_h^k \cdot \partial_\xi v_h d\xi \\ & + \int_{\mathbb{S}^1} I_h \left[f(l_h^{k-1}) n_h^{k-1} \cdot v_h \right] |\partial_\xi x_h^{k-1}|^2 d\xi = 0, \quad \forall v_h \in V_h, \end{aligned}$$

where $n_h^{k-1} = \left(\frac{\partial_\xi x_h^{k-1}}{|\partial_\xi x_h^{k-1}|} \right)^\perp$ is the unit normal vector. Through a straightforward computation, we find it can be written equivalently as

$$\alpha \frac{x_j^k - x_j^{k-1}}{\tau} + (1 - \alpha) \left(\frac{x_j^k - x_j^{k-1}}{\tau} \cdot n_j^{k-1} \right) n_j^{k-1} = \frac{2(x_{j+1}^k - 2x_j^k + x_{j-1}^k)}{(q_j^{k-1})^2 + (q_{j+1}^{k-1})^2} - f(l_h^{k-1}) n_j^{k-1}, \quad (6.3)$$

where $n_j^{k-1} = \left(\frac{x_j^{k-1} - x_{j-1}^{k-1}}{q_j^{k-1}} \right)^\perp$.

6.1 Accuracy test

To evaluate the convergence order of the proposed three schemes, we primarily consider the following cases of geometric flows with different initial curves:

Case 1: An ellipse initial curve, parameterized by $(2 \cos \theta, \sin \theta)^T$, $\theta \in [0, 2\pi]$, with the corresponding flow being the AP-CSF with $f(L) = 2\pi/L$;

Case 2: A four-leaf rose initial curve, parameterized by $(\cos(2\theta) \cos \theta, \cos(2\theta) \sin \theta)^T$, $\theta \in [0, 2\pi]$, with the corresponding flow being the AP-CSF for nonsimple curves with $f(L) = 2\pi \text{ind}/L$, $\text{ind}(\Gamma) = 3$;

Case 3: An ellipse initial curve, with the corresponding flow being a curve flow with area decreasing rate of π , i.e., $f(L) = (2\pi - \beta)/L$, $\beta = \pi$.

As the exact solutions of the above cases are unknown, we consider the following numerical errors for the FDM (6.1):

$$L_t^\infty H_G^1 \text{ error} \quad (\mathcal{E}_1)_{h,\tau}(T) := \max_{1 \leq k \leq T/\tau} \|x_{h,\tau}^k - \widehat{x}_{h/2,\tau/4}^{4k}\|_{H_G^1},$$

$$\text{Manifold distance} \quad (\mathcal{E}_2)_{h,\tau}(T) := M(\Gamma_{h,\tau}^{T/\tau}, \Gamma_{h/2,\tau/4}^{4T/\tau}),$$

where we view $\widehat{x}_{h/2,\tau/4}^{4k}$ as a grid function over \mathcal{G}_h with grid values $\{x_{2j}^{4k}\}_{j=1}^N$, and the L_G^∞ norm is defined as $\|g\|_{L_G^\infty} := \max_{j=1,\dots,N} |g_j|$. Furthermore, the polygons $\Gamma_{h,\tau}^{T/\tau}$ and $\Gamma_{h/2,\tau/4}^{4T/\tau}$ are the images of $x_{h,\tau}^{T/\tau}$ and $x_{h/2,\tau/4}^{4T/\tau}$, respectively.

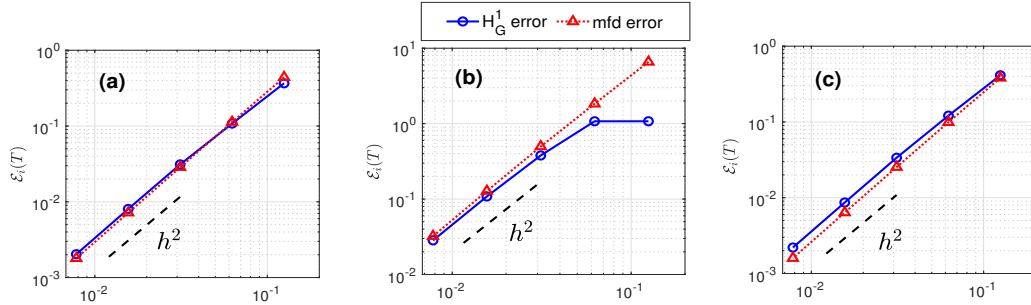


Figure 2: Numerical errors under different norms for the FDM (6.1) at $T = 1/4$: (a) Case 1; (b) Case 2; (c) Case 3.

Different types of errors for the FDM (6.1) are depicted Fig 2, where we choose $h = 2\pi/N$, $\tau = 0.5h^2$. The numerical results indicate that, for each instance of nonlocal flows listed above, the solution of (6.1) converges quadratically in $L_t^\infty L_G^2$, $L_t^\infty H_G^1$ and $L_t^\infty L_G^\infty$, which agrees with the theoretical results in Theorem 3.2. Moreover, we observe a quadratic convergence under the manifold distance, aligning with the theoretical findings in Corollary 5.2 (1).

We now turn to the convergence order test of the FEM (6.2) and the FEM-TM (6.3). We

similarly consider the following numerical errors

$$L_t^\infty H_x^1 \text{ error} \quad (\mathcal{E}_3)_{h,\tau}(T) := \max_{1 \leq k \leq T/\tau} \left(\|x_{h,\tau}^k - x_{h/2,\tau/4}^{4k}\|_{L^2(\mathbb{S}^1)} + \|\partial_\xi x_{h,\tau}^k - \partial_\xi x_{h/2,\tau/4}^{4k}\|_{L^2(\mathbb{S}^1)} \right),$$

$$\text{Manifold distance} \quad (\mathcal{E}_4)_{h,\tau}(T) := M(\Gamma_{h,\tau}^{T/\tau}, \Gamma_{h/2,\tau/4}^{4T/\tau}),$$

where $x_{h,\tau}^k$ represents the solution obtained by the above fully discrete scheme (6.2) or (6.3) with mesh size h and time step τ .

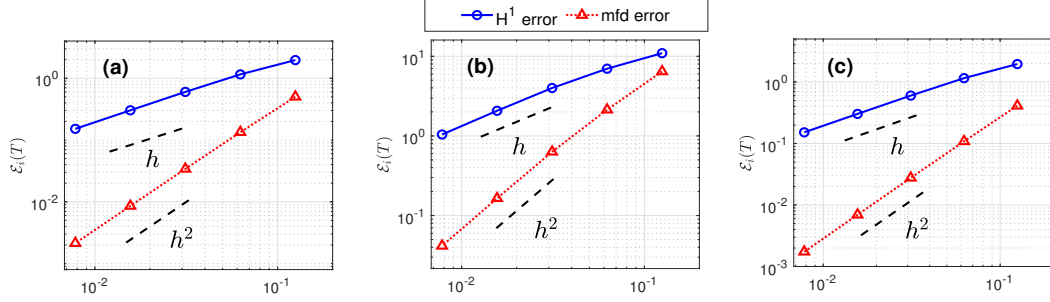


Figure 3: Numerical errors under different norms of the FEM (6.2) at $T = 1/4$: (a) Case 1; (b) Case 2; (c) Case 3.

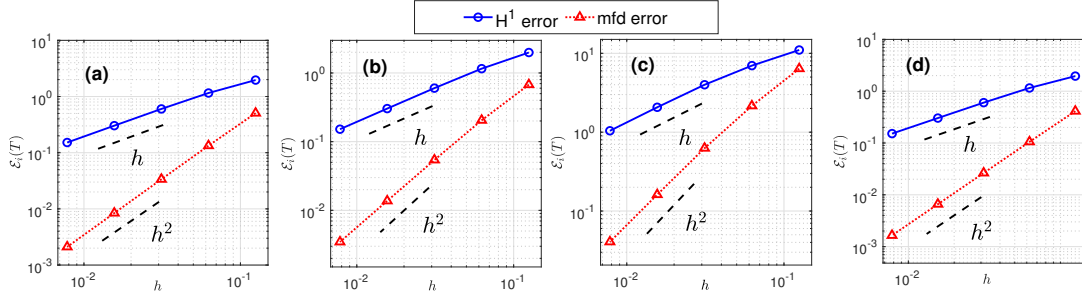


Figure 4: Numerical errors under different norms of the FEM-TM (6.3) at $T = 1/4$: (a) Case 1 with $\alpha = 1$; (b) Case 1 with $\alpha = 0.5$; (c) Case 2 with $\alpha = 1$; (d) Case 3 with $\alpha = 1$.

The numerical errors of the FEM (6.2) and the FEM-TM (6.3) are presented in Fig 3 and Fig 4, respectively, from which we observe that, for each nonlocal flow with ind and β , the solution of (6.2) and (6.3) converge linearly in $L_t^\infty H_x^1$, consistent with the theoretical results in Theorems 4.3 and 4.6. Moreover, Fig 4 (a) and (b) illustrate that the scheme (6.3) performs equally well for different choices of α . Additionally, we observe that the solution converges quadratically under the manifold distance, which is superior to the theoretical results in Corollary 5.2 (2) and (3).

6.2 Dynamics and evolution of geometric quantities

In this subsection, we utilize the proposed three methods: FDM (6.1), FEM (6.2) and FEM-TM (6.3) to simulate the nonlocal geometric flows. We are mainly concerned with the evo-

lution of the following geometric quantities: perimeter $L(t)$, relative area loss $\Delta A(t)$ and the mesh ratio function $\Psi(t)$ defined as

$$L(t)|_{t=t_k} = l_h^k, \quad \Delta A(t)|_{t=t_k} = \frac{A_h^k - A_h^0}{A_h^0}, \quad \Psi(t)|_{t=t_k} = \frac{\max_{j=1,\dots,N} q_j^k}{\min_{j=1,\dots,N} q_j^k},$$

where l_h^k and A_h^k are the perimeter and the area of the polygon determined by x_h^k , respectively, and $q_j^k = |x_j^k - x_{j-1}^k|$. Note that for the area of an immersed curve, such as the four-leaf rose, it is treated as a signed area. In morphological evolutions, we primarily focus on the following cases:

Case 1: A flower initial curve parametrized by

$$((2 + \cos(6\theta)) \cos \theta, (2 + \cos(6\theta)) \sin \theta)^T, \quad \theta \in [0, 2\pi],$$

with the corresponding flow being the AP-CSF with $f(L) = 2\pi/L$;

Case 2: A four-leaf rose initial curve, with the corresponding flow being the AP-CSF for nonsimple curve with $f(L) = 2\pi \text{ind}/L$, $\text{ind}(\Gamma) = 3$;

Case 3: A 4×1 rectangular initial curve with the corresponding flow being a curve flow with area decreasing rate of π , i.e., $f(L) = (2\pi - \beta)/L$, $\beta = \pi$.

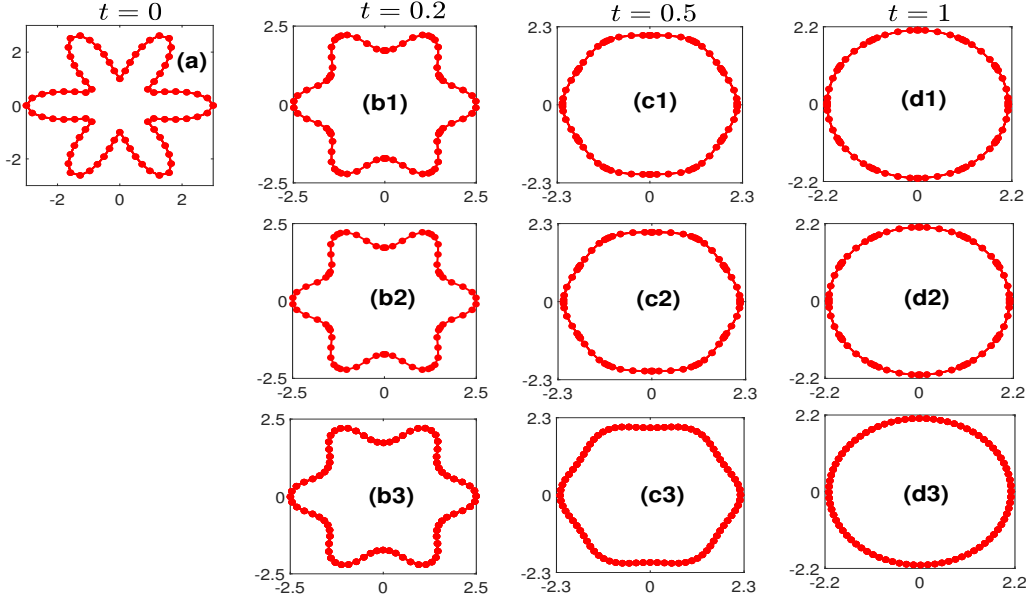


Figure 5: Snapshots of the curve evolution using the FDM (first row), FEM (second row) and FEM-TM (third row) with $\alpha = 1$ for Case 1. The parameters are chosen as $N = 80$ and $\tau = 1/160$.

Figs. 5-8 depict the comparisons of the three schemes through the evolutions of the solution and geometric quantities for the respective three cases. Here we fix the number of nodes $N = 80$ and the time step $\tau = 1/160$. Based on the observations from Figs. 5-8, we can draw the following conclusions:

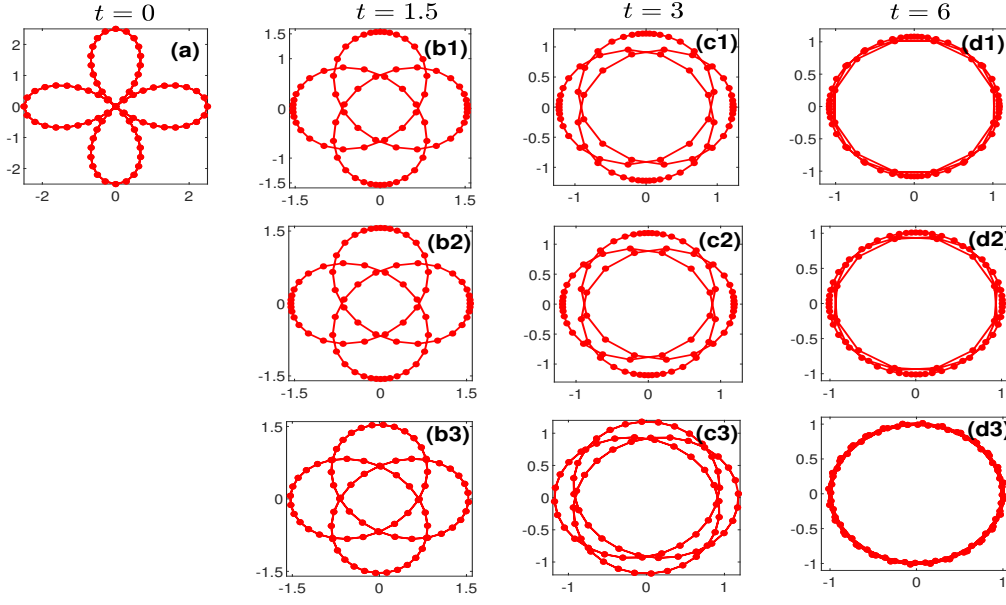


Figure 6: Snapshots of the curve evolution using the FDM (first row), FEM (second row) and FEM-TM (third row) with $\alpha = 1$ for Case 2. The parameters are chosen as $N = 80$ and $\tau = 1/160$.

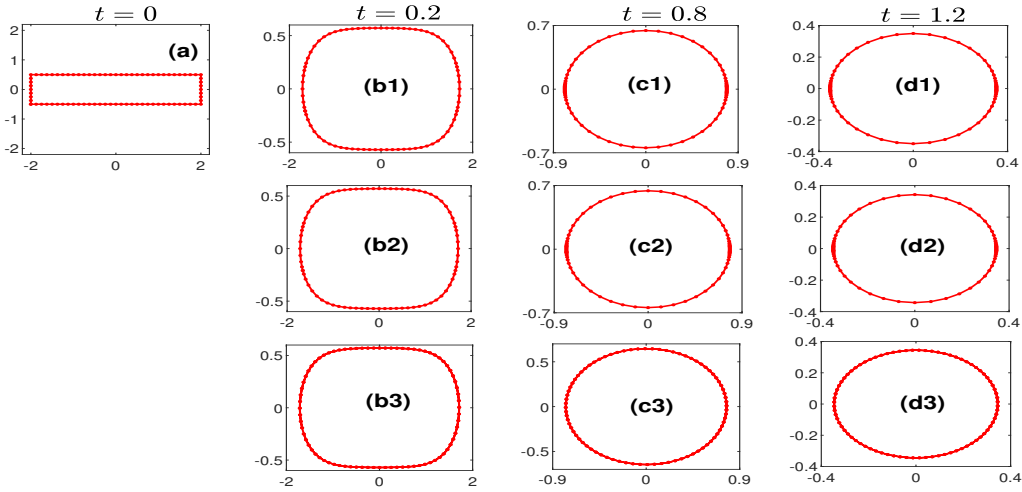


Figure 7: Snapshots of the curve evolution using the FDM (first row), FEM (second row) and FEM-TM (third row) with $\alpha = 1$ for Case 3. The parameters are chosen as $N = 80$ and $\tau = 1/160$.

- (i) All of the schemes can evolve the above three cases successfully into their equilibria, i.e., circle for Case 1, triple circle for Case 2, and a round point for Case 3, which agrees with the theoretical results in [41] (cf. Figs. 5, 6 and 7).
- (ii) For Case 1 and Case 2, the area is conserved numerically up to some precision while the area is decreasing numerically with the rate π for Case 3 (cf. Fig. 8 (b)).
- (iii) As demonstrated in Fig. 8 (c), the FEM-TM redistributes the points during the evolution and ultimately achieves the equidistribution property, i.e., $\Psi(t) \rightarrow 1$ as $t \rightarrow +\infty$. This coincides the motivation in Section 4.2. In contrast, the FDM and the FEM fail to preserve good mesh quality during the evolution.

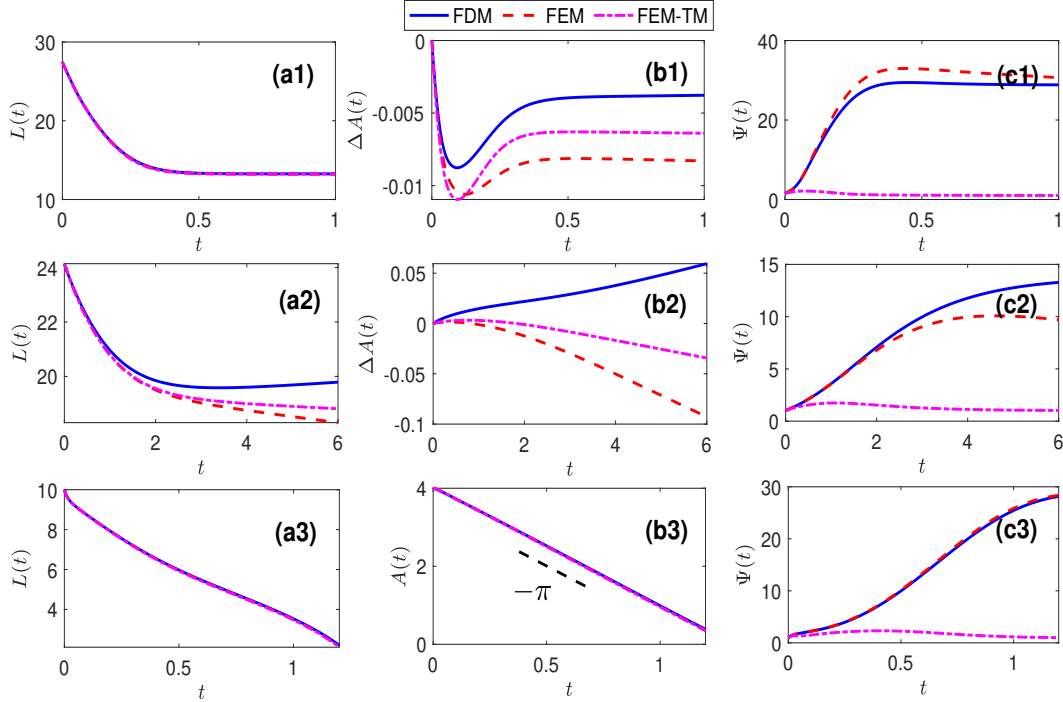


Figure 8: Evolution of the geometric quantities using the FDM, FEM and FEM-TM with $\alpha = 1$ for Cases 1-3 is illustrated in the first through third rows, respectively. (a) Perimeter $L(t)$; (b) Relative area loss $\Delta A(t)$; (c) Mesh ratio function $\Psi(t)$. The parameters are chosen as $N = 80$ and $\tau = 1/160$.

We close this section with a numerical example to demonstrate that the parameter α in the FEM-TM (6.3) signifies the velocity of tangential motions. We conduct simulations for Case 1 using the FEM-TM with varying values $\alpha = 0.1, 0.5$ and 1 . As depicted in Fig. 9 (c), a smaller α leads to a more effective redistribution of the mesh points. Fig. 9 (b) illustrates that as α approaches 0, the loss of area becomes greater. This indicates that for a fixed set of computational parameters N and τ , a smaller value of α yields a less accurate simulation, aligning with the findings in Theorem 4.6, wherein the exponential of $\frac{1}{\alpha}$ is involved in the error estimate.

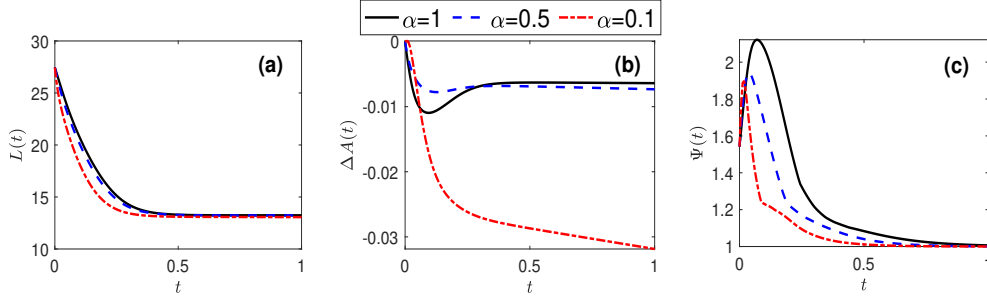


Figure 9: Evolution of geometric quantities using the the FEM-TM with different $\alpha = 0.1, 0.5, 1$ for Case 1. (a) Perimeter $L(t)$; (b) Relative area loss $\Delta A(t)$; (c) Mesh ratio function $\Psi(t)$. The parameters are chosen as $N = 80$ and $\tau = 1/160$.

7 Conclusions

We developed three distinct semi-discrete schemes for simulating some nonlocal geometric flows involving perimeter and the corresponding error estimates were established. Specifically, the FDM exhibits quadratic convergence in H^1 , whereas the FEM and the FEM-TM are convergent at the first order in H^1 . Furthermore, all three methods demonstrate robust quadratic convergence under manifold distance. Extensive numerical experiments have underscored the superior mesh quality of the FEM-TM compared to FDM and FEM.

It is noteworthy that our proof of the error estimate under manifold distance is not optimal for FEM-TM and FEM. Exploring the possibility of providing a proof of optimal convergence for piecewise linear finite element would be a valuable endeavor.

Acknowledgments

W. Jiang was supported by the National Natural Science Foundation of China Grant (No. 12271414) and the Natural Science Foundation of Hubei Province Grant (No. 2022CFB245), and C. Su and G. Zhang were supported by National Key R&D Program of China (Grant No. 2023Y-FA1008902) and the National Natural Science Foundation of China Grant (No. 12201342).

References

- [1] G. Bai and B. Li. A new approach to the analysis of parametric finite element approximations to mean curvature flow. *Found. Comput. Math.*, doi.org/10.1007/s10208-023-09622-x, 2023.
- [2] E. Bänsch, K. Deckelnick, H. Garcke, and P. Pozzi. *Interfaces: modeling, analysis, numerics. Oberwolfach Seminar, Volume 51*. Birkhäuser, Springer, 2023.
- [3] E. Bänsch, P. Morin, and R. Nochetto. A finite element method for surface diffusion: The parametric case. *J. Comput. Phys.*, **203**:321–343, 2005.

- [4] W. Bao, W. Jiang, and Y. Li. A symmetrized parametric finite element method for anisotropic surface diffusion of closed curves. *SIAM J. Numer. Anal.*, **61**(2):617–641., 2023.
- [5] W. Bao and Q. Zhao. A structure-preserving parametric finite element method for surface diffusion. *SIAM J. Numer. Anal.*, **59**(5):2775–2799., 2021.
- [6] J. W. Barrett, H. Garcke, and R. Nürnberg. Parametric finite element method approximations of curvature driven interface evolutions. In Andrea Bonito and Ricardo H. Nochetto, editors, *Handbook of Numerical Analysis, Volume 21*, pages 275–423. Elsevier, 2020.
- [7] L. Bronsard and B. Stoth. Volume-preserving mean curvature flow as a limit of a nonlocal Ginzburg-Landau equation. *SIAM J. Math. Anal.*, **28**(4):769–807., 1997.
- [8] A. Chambolle, M. Morini, and M. Ponsiglione. Nonlocal curvature flows. *Arch. Ration. Mech. Anal.*, **218**:1263–1329., 2015.
- [9] M. C. Dallaston and S. W. McCue. An accurate numerical scheme for the contraction of a bubble in a Hele-Shaw cell. *The ANZIAM Journal*, **54**:C309–C326, 2012.
- [10] M. C. Dallaston and S. W. McCue. Bubble extinction in Hele-Shaw flow with surface tension and kinetic undercooling regularization. *Nonlinearity*, **26**(6):1639–1665., 2013.
- [11] M. C. Dallaston and S. W. McCue. A curve shortening flow rule for closed embedded plane curves with a prescribed rate of change in enclosed area. *Proc. R. Soc. A*, **472**(2185):20150629, 2016.
- [12] K. Deckelnick and G. Dziuk. On the approximation of the curve shortening flow. *Pitman Research Notes in Mathematics Series*, pages 100–108., 1995.
- [13] K. Deckelnick, G. Dziuk, and C. M. Elliott. Computation of geometric partial differential equations and mean curvature flow. *Acta Numer.*, **14**:139–232., 2005.
- [14] K. Deckelnick and R. Nürnberg. Discrete anisotropic curve shortening flow in higher codimension. *arXiv:2310.02138*, 2023.
- [15] K. Deckelnick and R. Nürnberg. Discrete hyperbolic curvature flow in the plane. *SIAM J. Numer. Anal.*, **61**:1835–1857., 2023.
- [16] K. Deckelnick and R. Nürnberg. A novel finite element approximation of anisotropic curve shortening flow. *Interfaces Free Bound.*, **4**:671–708, 2023.
- [17] K. Deckelnick and R. Nürnberg. An unconditionally stable finite element scheme for anisotropic curve shortening flow. *Arch. Math.*, **59**:263–274., 2023.
- [18] K. Deckelnick and R. Nürnberg. Finite element schemes with tangential motion for fourth order geometric curve evolutions in arbitrary codimension. *arXiv:2402.16799*, 2024.

- [19] do Carmo M. P. *Differential Geometry of Curves and Surfaces*. Dover Publications, Inc., Mineola, NY, 2016.
- [20] B. Duan and B. Li. New artificial tangential motions for parametric finite element approximation of surface evolution. *SIAM J. Sci. Comput.*, **46**:A587–A608, 2024.
- [21] G. Dziuk. Discrete anisotropic curve shortening flow. *SIAM J. Numer. Anal.*, **36**(6):1808–1830., 1999.
- [22] C. M. Elliott and H. Fritz. On approximations of the curve shortening flow and of the mean curvature flow based on the DeTurck trick. *IMA J. Numer. Anal.*, **37**(2):543–603., 2017.
- [23] M. Gage. On an area-preserving evolution equation for plane curves. *Contemp. Math.*, **51**:51–62., 1986.
- [24] S. F. Vita I. C. Dolcetta and R. March. Area-preserving curve-shortening flows: from phase separation to image processing. *Interfaces Free Bound.*, **4**(4):325–343., 2002.
- [25] L. Jiang and S. Pan. On a non-local curve evolution problem in the plane. *Comm. Anal. Geom.*, **16**(1):1–26., 2008.
- [26] W. Jiang, C. Su, and G. Zhang. A convexity-preserving and perimeter-decreasing parametric finite element method for the area-preserving curve shortening flow. *SIAM J. Numer. Anal.*, **61**(4):1989–2010., 2023.
- [27] W. Jiang, C. Su, and G. Zhang. A second-order in time, BGN-based parametric finite element method for geometric flows of curves. *arXiv:2309.12875*, 2023.
- [28] W. Jiang, C. Su, and G. Zhang. Stable BDF time discretization of BGN-based parametric finite element methods for geometric flows. *arXiv:2402.03641*, 2024.
- [29] U. F. Mayer. A numerical scheme for moving boundary problems that are gradient flows for the area functional. *European J. Appl. Math.*, **11**(1):61–80., 2000.
- [30] K. Mikula and D. Ševčovič. Computational and qualitative aspects of evolution of curves driven by curvature and external force. *Comput. Vis. Sci.*, **6**(4):211–225., 2004.
- [31] K. Mikula and D. Ševčovič. A direct method for solving an anisotropic mean curvature flow of plane curves with an external force. *Math. Methods Appl. Sci.*, **27**(13):1545–1565., 2004.
- [32] L. Pei and Y. Li. A structure-preserving parametric finite element method for area-conserved generalized mean curvature flow. *J. Sci. Comput.*, **96**(6):1–21, 2023.
- [33] P. Pozzi and B. Stinner. Convergence of a scheme for elastic flow with tangential mesh movement. *ESAIM Math. Model. Numer. Anal.*, **57**(2):445–466, 2023.

- [34] S. J. Ruuth and B. Wetton. A simple scheme for volume-preserving motion by mean curvature. *J. Sci. Comput.*, **19**:373–384., 2003.
- [35] G. Sapiro. *Geometric Partial Differential Equations and Image Analysis*. Cambridge University Press, 2001.
- [36] G. Sapiro and A. Tannenbaum. Area and length preserving geometric invariant scale-spaces. *IEEE Trans. Pattern Anal. Mach. Intell.*, **17**:67–72, 1995.
- [37] D. Ševčovič and K. Mikula. Evolution of plane curves driven by a nonlinear function of curvature and anisotropy. *SIAM J. Appl. Math.*, **61**(5):1473–1501., 2001.
- [38] D. Tsai and X. Wang. On length-preserving and area-preserving nonlocal flow of convex closed plane curves. *Calc. Var. Partial Differential Equations*, **54**:3603–3622., 2015.
- [39] D. Tsai and X. Wang. The evolution of nonlocal curvature flow arising in a Hele-Shaw problem. *SIAM J. Math. Anal.*, **50**(1):1396–1431., 2018.
- [40] T. Ushijima and S. Yazaki. Convergence of a crystalline approximation for an area-preserving motion. *J. Comput. Appl. Math.*, **166**(2):427–452., 2004.
- [41] X. Wang and L. Kong. Area-preserving evolution of nonsimple symmetric plane curves. *J. Evol. Equ.*, **14**(2):387–401., 2014.
- [42] Q. Zhao, W. Jiang, and W. Bao. An energy-stable parametric finite element method for simulating solid-state dewetting. *IMA J. Numer. Anal.*, **41**(3):2026–2055., 2021.